Journal of Control, Automation and Electrical Systems (2020) 31:1348–1374
https://doi.org/10.1007/s40313-020-00633-5

Observability of Network Systems: A Critical Review of Recent Results

Arthur N. Montanari[1] · **Luis A. Aguirre**[2]

Received: 13 December 2019 / Revised: 28 July 2020 / Accepted: 4 August 2020 / Published online: 24 August 2020

Abstract
Observability is a property of a dynamical system that defines whether or not it is possible to reconstruct the trajectory temporal evolution of the internal states of a system from a given set of outputs (measurements). In the context of network systems, two important goals are: (i) to determine if a given set of sensor nodes is sufficient to render the network observable; and (ii) what is the best set of sensor nodes among different available combinations that provide a more accurate state estimation of the network state. Alongside Kalman's classical definition of observability, a graph-theoretical approach to determine the observability of a network system has gathered a lot of attention in the literature despite several following works showing that, under certain circumstances, this kind of approach might underestimate, for practical purposes, the required number of sensor nodes. In this work, we review with a critical mindset the literature of observability of dynamical systems, counterpoising the pros and cons of different approaches in the context of network systems. Some future research directions for this field are discussed and application examples in power grids and multi-agent systems are shown to illustrate our main conclusions.

Keywords Observability · Dynamical systems · Network systems · Sensor placement

1 Introduction

The mathematical modeling of *dynamical systems* is a fundamental framework in engineering that provides a means to analyze aspects of a system, such as its stability, controllability or observability, and thereafter design control laws for practical applications (Chen 1999; Khalil 2002). However, being designed for the most part with systems of low-dimensional order in mind, classic control theory methods are not efficient, or even feasible, for large-scale systems, such as interconnected (networked) dynamical systems. This practical limitation has led control theory notions to be adapted, optimized, or even redefined, in the literature for high-dimensional applications (Chen 2014).

A specific, but recurrent, type of high-dimensional system can be defined as *networks*. A network is a set of nodes interconnected by edges, in which information flows among its elements through pairwise interactions. It can be mathematically modeled by graph structures, which allow a wide range of useful metrics and algorithms of graph theory (Newman 2010; Chen et al. 2013; Bullo 2016). For instance, graph theory can be used to assess the robustness to spreading failures in power systems (Zhang et al. 2014; Schäfer et al. 2018) or biological networks (Schimit and Monteiro 2009; Gilarranz et al. 2017).

Up to the end of the twentieth century, it was believed that real-world interconnected systems, such as neuronal, social, communication, traffic, and energy networks, and even the Internet, were composed of stochastic connections among its nodes. However, works over the last two decades highlighted that most of real-world networks share similar topological characteristics—not being purely random, nor purely regular (Watts and Strogatz 1998; Barabási 1999, 2009). *Complex networks*, therefore, are a subclass of mathematical models derived from graph theory, in which topological structures (graphs) show recurrent patterns that are found in the most diverse real networks present in nature and engineering (Chen et al. 2013; Barabási and Pósfasi 2016). Based on these findings, the last years have been flooded with studies about complex networks models, such as *scale-free networks*

✉ Arthur N. Montanari
montanariarthur@gmail.com

Luis A. Aguirre
aguirre@ufmg.br

[1] Graduate Program in Electrical Engineering of the Universidade Federal de Minas Gerais (UFMG), Av. Antônio Carlos 6627, 31270-901 Belo Horizonte, Minas Gerais, Brazil

[2] Depto. de Engenharia Eletrônica, UFMG, Belo Horizonte, Brazil

(Barabási 1999) and *small-world networks* (Watts and Strogatz 1998).

The study of complex networks is essential to increase the knowledge about the structural characteristics and recurrent patterns that govern real networks—even when nodal dynamics are disregarded in favor of a higher focus on the graph properties. It is a first step in a long ladder whose final goal is to develop control techniques for *dynamical complex networks* (Wang and Chen 2003). *Dynamical networks* are defined by a set of dynamical systems that, when analyzed individually, describe relatively simpler behaviors, but, when interconnected, develop interactions that considerably raise the system complexity (Monteiro 2014). This is a consequence of a twofold interaction between local properties (nodal dynamics) and global properties, such as the network structure or topology (Aguirre et al. 2018).

Many mathematical models were expanded to include complex networks that describe the spatial relations and interactions between their elements. Among the numerous examples are: models of infectious diseases (Moreno et al. 2002; Schimit and Monteiro 2009), reaction-diffusion systems (Wolfrum 2012) (e.g., predator-prey models (Nakao and Mikhailov 2010)), and Boolean systems (Gates and Rocha 2015). In the field of nonlinear dynamics, the study of synchronization in networks of oscillators stands out (Boccaletti et al. 2002; Arenas et al. 2008; Rodrigues et al. 2016), with important applications in power systems (Dorfler et al. 2013) and biological networks (Hammond et al. 2007). In this case, each node is composed of an individual dynamical system, a nonlinear oscillator, and its interactions are determined by coupling functions of the state variables of different oscillators. Usually, the main goal is to determine under which conditions the synchronization manifold of a dynamical network of oscillators becomes stable. These conditions can be related to the network structure (Wang and Chen 2002; Moreno and Pacheco 2004), the coupling method (Stankovski et al. 2017), or the nonlinear oscillator model—from the well-studied Kuramoto phase oscillator (Kuramoto 1975; Dorfler and Bullo 2014) to chaotic ones (Boccaletti et al. 2002; Eroglu et al. 2017).

Observability is a measure that determines if the trajectory temporal evolution of the internal states of a dynamical system can be reconstructed based on knowledge of the inputs and outputs, as introduced by Kalman (1959). This classic concept of observability, addressed here as *structural observability*, is based on a *crisp* definition, i.e., the system is or is not observable (Chen 1999). This crisp classification might be misleading since, in some *ill-conditioned* cases, a small change in the parameter space of an unobservable dynamical system might make it observable, and vice versa (Friedland 1975). Thus, although observability is a sufficient and necessary condition for the design of a stable state observer (Luenberger 1966), a more important question for practical purposes might be whether a system is *almost unobservable* or not.

This structural definition can be extended by metrics that quantify observability in a gradual or continuous manner, i.e., measuring *how well* the system trajectory can be reconstructed (Friedland 1975; Aguirre 1995), which we address as *dynamical observability*. Dynamical observability not only allows one to identify if a given dynamical system is observable from a practical point-of-view, but it also allows one to quantify and rank the degree of observability conveyed by different sets of output measures—and therefore choose the best option (Letellier et al. 1998).

In the context of network systems, it is a reasonable assumption that not all nodes are available for measurement. For instance, not every single neuron of the one hundred billion neurons present in the brain are physically accessible for direct measurement. Likewise, it might not be economically viable to place a phasor measurement unit in every single electrical substation of a power system. Thus, two important goals in the field of network systems are: (i) to determine if a given set of sensor nodes[1] renders the network observable, a problem that can be assessed by *structural observability* metrics; and (ii) to determine the *best* (or minimum) set of sensor nodes from different configurations, a problem that can only be solved by *dynamical observability* metrics. Indeed, the optimal sensor placement problem can be approached as an observability problem.

However, classical observability metrics from control theory are unfeasible for high-dimensional (network) systems. To circumvent this issue, Liu et al. (2011) presented a pioneer work on the controllability of network systems,[2] where the notion of network controllability is revisited under a different definition grounded on graph theory (Lin 1974), which we address here as *topological controllability and observability*. This opened a recent and new branch for research in the control of (complex) network systems (Liu and Barabási 2016), which has gathered several—but not yet consolidated—results in the literature.

Contributions Undoubtedly, many works in the literature embraced the graph-theoretical approach to the controllability and observability of network systems (Pósfai et al. 2013; Jia et al. 2013; Nacher and Akutsu 2013; Gao et al. 2014; Yan

[1] A common jargon in the literature is to refer to nodes available for measurement (that issue output signals) as *sensor nodes*, and control nodes (that have input signals) as *driver nodes*.

[2] The study of controllability and observability of network systems was born in a controllability context. Thus, some of the discussion in this work might be focused on controllability rather than observability, although we can rely on the duality between both concepts (in a linear context) to understand and compare the available results.

et al. 2015; Leitold et al. 2017), leading to some major developments in this field, such as applications in the control of neuronal networks (Gu et al. 2015; Su et al. 2017). This preference for the graph-theoretical perspective of observability, developed by Lin (1974), is mainly due to the intuitive representation of network systems by graph models and the high scalability of graph metrics.

However, it must be noted that a great number of results in this field totally disregard the effects of nodal dynamics. This led to recurrent criticism on the true applicability of their work (Cowan et al. 2012; Gates and Rocha 2015; Wang et al. 2017; Leitold et al. 2017), as upcoming works showed that the topological observability severely underestimates the required number of sensor nodes for practical purposes such as state estimation (Haber et al. 2018; Montanari and Aguirre 2019). Not only that, but the conclusions might be drastically different when the effects of nonlinearity are properly taken into account (Motter 2015; Letellier et al. 2018; Jiang and Lai 2019).

Thus, the main contribution of this work is not only to survey the literature of observability of network systems—which has been done before by Liu and Barabási (2016)—but mainly to review, with a critical mindset, recent advances on the observability of network systems from a control theory perspective. To that end, we also revisit the basic concepts of observability of linear and nonlinear low-dimensional dynamical systems. The pros and cons of a topological approach to the observability of network systems are exposed. To confront the concepts of structural, dynamical and topological observability at a "practical" level, we provide two application examples of optimal sensor placement in the context of power systems and multi-agent system consensus.

Despite the recent contributions in this field, the interplay between the observability of network systems and the effects of nodal dynamics and network topology is still an open question in the literature. Thus, we also present in this work some interesting guidelines for future research in the observability of network systems that are mostly grounded on control theory rather than on graph theory.

Outline This work is organized as follows. Section 2 defines the notation for state-space and graph representation as well as presents some background on modeling of dynamical networks. Sections 3, 4 and 5 present and discuss, respectively, the concepts of structural, dynamical, and topological observability for linear and nonlinear dynamical systems. Section 6 critically reviews the literature of observability (and controllability) of network systems, while Sect. 7 provides some guidelines and future research directions in this field of work. Section 8 describes two application examples in power systems and multi-agent systems. Finally, Sect. 9 concludes this work.

2 Dynamical Networks Modeling

A *dynamical network* can be studied at three levels: (i) the *node dynamics*, described by a dynamical system; (ii) the *network topology*, described by a graph; and (iii) the *full network*, a combination of both aforementioned levels (Aguirre et al. 2018). The interconnection among independent and comparatively simpler dynamical systems in a network unravels different kinds of interactions that considerably raises the system complexity (Monteiro 2014). Thus, to investigate a full network, three components must be considered: (i) the graph, which describes the interconnection structure along the network; (ii) the coupling method, which describes how these interconnections unfold; and (iii) the node dynamics, which describes the behavior and interactions of a node when isolated from its neighborhood.

Section 2.1 formalizes the adopted notation for dynamical systems and graph theory, while Sect. 2.2 presents how a dynamical network can be represented based on the three aforementioned components.

2.1 Notation

Dynamical Systems The state-space representation of a linear continuous time-invariant dynamical system is given by

$$\begin{cases} \dot{\boldsymbol{x}} = A\boldsymbol{x} + B\boldsymbol{u}, \\ \boldsymbol{y} = C\boldsymbol{x} + D\boldsymbol{u}, \end{cases} \tag{1}$$

where $\boldsymbol{x} \in \mathbb{R}^n$ is the state vector, $\boldsymbol{u} \in \mathbb{R}^p$ is the input (control) vector, $\boldsymbol{y} \in \mathbb{R}^q$ is the output (measurement) vector, and (A, B, C, D) are matrices of consistent dimensions known as, respectively, the dynamic matrix, input (control) matrix, output (measurement) matrix and feedforward matrix. Time t dependence is omitted for compactness of notation, only for the system variables $\boldsymbol{x}$, $\boldsymbol{u}$ and $\boldsymbol{y}$. Vectors are defined as column vectors, denoted by bold lower-case letters, and matrices by upper-case letters.

For an autonomous nonlinear continuous time-invariant dynamical system, the state-space representation is:

$$\begin{cases} \dot{\boldsymbol{x}} = \boldsymbol{f}(\boldsymbol{x}), \\ \boldsymbol{y} = \boldsymbol{h}(\boldsymbol{x}), \end{cases} \tag{2}$$

where $\boldsymbol{f} : \mathcal{M} \mapsto \mathcal{M}$ and $\boldsymbol{h} : \mathcal{M} \mapsto \mathbb{R}^q$ are nonlinear functions, and $\boldsymbol{x} \in \mathcal{M} \subseteq \mathbb{R}^n$. It is assumed that the reader is familiar with linear and nonlinear system theory. For more details, the reader is referred to (Chen 1999) for linear systems theory, and to (Vidyasagar 1978; Khalil 2002) for fundamentals of nonlinear systems.

Graph A *graph* is defined as $\mathcal{G} = \{\mathcal{V}, \mathcal{E}\}$, where $\mathcal{V} = \{v_1, \ldots, v_m\}$ and $\mathcal{E} \subseteq \mathcal{V} \times \mathcal{V} = \{e_1, \ldots, e_{\bar{m}}\}$ are finite sets

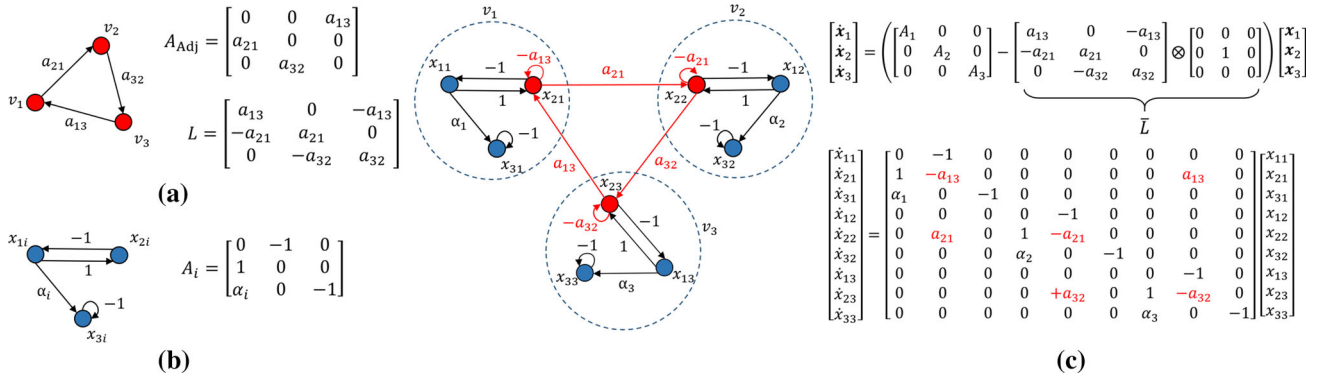

Fig. 1 **a** Network topology graph $\mathcal{G}$, and respective adjacency matrix A_{adj} and Laplacian matrix L. **b** Nodal dynamical system graph $\mathcal{G}_i$, for $i = 1, 2, 3$, of a 3-dimensional linear oscillator $\mathcal{X}_i = \{x_{1i}, x_{2i}, x_{3i}\}$, and respective dynamical matrix A_i. **c** Full network graph $\mathcal{G}_{\text{full}}$ of a network topology graph described in (**a**), where each node is composed of a linear oscillator presented in (**b**) coupled by the x_{2i} variable

of m nodes and $\bar{m}$ edges, respectively. The *cardinality* of a set, denoted by $|\mathcal{V}|$, is the number of elements of the set. The *adjacency matrix* A_{adj} is a representation that associates elements (edges) of $\mathcal{E}$ to a pair of elements (nodes) of $\mathcal{V}$. In what follows, the notation $A_{\text{adj}} = [a_{ij}]$ will be used to denote that a_{ij} is an entry of A_{adj}. For some conventions and properties of graph theory applied throughout this work, we refer the reader to "Appendix A".

2.2 Representation of Dynamical Networks

A *dynamical network* is a set of dynamical systems interconnected according to a network topology described by A_{adj}. Although the individual dynamical systems at nodes are relatively simple, the interactions among them considerably raises the network complexity. This interplay is not only governed by the nodal dynamics and the adjacency matrix, but also by the coupling method. In this section, we show how dynamical networks can be mathematically represented from a graph approach and a dynamic systems approach.

Graph Representation A network system can be described by a graph $\mathcal{G}$ which determines the interconnection structure among every element of $\mathcal{V}$, that is, the network topology. To $\mathcal{G}$, we associate $A_{\text{adj}} \in \mathbb{R}^{m\times m}$. In the case of a dynamical network, each node v_i is composed of a dynamical system (A_i, B_i, C_i, D_i) which itself can be represented by a graph $\mathcal{G}_i = \{\mathcal{X}_i, \mathcal{E}_i\}$. In this case, the adjacency matrix of $\mathcal{G}_i$ is the corresponding dynamical matrix $A_i \in \mathbb{R}^{n_i\times n_i}$. Hence, every node in $\mathcal{G}$ is expanded as a subgraph $\mathcal{G}_i$ and, therefore, the *full network* is represented by a larger and more complex graph $\mathcal{G}_{\text{full}} = \{\mathcal{V}_{\text{full}}, \mathcal{E}_{\text{full}}\}$ (and corresponding adjacency matrix $A^{\text{full}}_{\text{adj}} \in \mathbb{R}^{N\times N}$, where $N = \sum_{i=1}^{m} n_i$).

We illustrate this representation in Fig. 1. Consider a network of $m = 3$ nodes whose topology is described by a graph $\mathcal{G} = \{\mathcal{V}, \mathcal{E}\}$ (Fig. 1a). Consider that each node $v_i \in \mathcal{V}$ represents a 3-dimensional linear dynamical system $(A_i, 0, 0, 0)$, with its corresponding graph $\mathcal{G}_i$ illustrated in Fig. 1b. The full network $\mathcal{G}_{\text{full}}$ (Fig. 1c) is, therefore, given by $\mathcal{G}$, where each element of $\mathcal{V}$ is expanded as a subgraph $\mathcal{G}_i$. In this case, graphs $\{\mathcal{G}_1, \mathcal{G}_2, \mathcal{G}_3\}$ are subgraphs of $\mathcal{G}_{\text{full}}$ (however, this is not always the case, as seen in Example 1).

Not only expanding each node as a subgraph is essential since it includes the effects of nodal dynamics in the representation, but it also highlights which is the coupling variable between the interconnected nodes. Albeit for higher dimensionality ($|\mathcal{G}_{\text{full}}| = N$), it is clear that the full network representation is a more complex and complete model of the dynamical network, which can potentially lead to a more reliable analysis of the system.

State-Space Representation A dynamical network can also be represented as a larger dynamical system (1) of higher-dimensionality $N = \sum_{i=1}^{m} n_i$, where n_i is the dimension of the i-th nodal dynamical system and m is the cardinality of the network topology $\mathcal{G}$. This high-dimensional representation, however, is usually detrimental to classical methods from system analysis and control design (Chen 2014). Nevertheless, a dynamical network is a special case of a high-dimensional system. Since many applications in network systems have a rather sparse network topology and similar nodal dynamics (same set of ODEs but with parametric differences, yielding $N = mn$, where $n_i = n, \forall i$), it is in the best interest of analysis and control methods of dynamical networks to take advantage of these properties.

In this sense, a compact state-space representation of a *full (dynamical) network* is presented in what follows, adapted from the work of Pecora and Carroll (1998):

$$\begin{bmatrix} \dot{\boldsymbol{x}}_1 \\ \dot{\boldsymbol{x}}_2 \\ \vdots \\ \dot{\boldsymbol{x}}_m \end{bmatrix} = \left(\begin{bmatrix} A_1 & 0 & \dots & 0 \\ 0 & A_2 & \dots & 0 \\ \vdots & \vdots & \ddots & \vdots \\ 0 & 0 & \dots & A_m \end{bmatrix} - \bar{L} \right) \begin{bmatrix} \boldsymbol{x}_1 \\ \boldsymbol{x}_2 \\ \vdots \\ \boldsymbol{x}_m \end{bmatrix}, \tag{3}$$

where $\boldsymbol{x} = [\boldsymbol{x}_1^\mathsf{T} \ \dots \ \boldsymbol{x}_m^\mathsf{T}]^\mathsf{T} \in \mathbb{R}^N$ and $\boldsymbol{x}_i = [x_{1i} \ \dots \ x_{ni}]^\mathsf{T} \in \mathbb{R}^n$, for $i = 1, \dots, m$. Thus, x_{ji} is the j-th state variable of the dynamical system at node v_i, and $\boldsymbol{x}_i$ is the corresponding state vector. $\bar{L}$ is the Laplacian matrix of the full network $\mathcal{G}_{\text{full}}$, describing the connection among all the state variables. The negative sign before $\bar{L}$ implies that the state variables are diffusively coupled.[3]

The Laplacian matrix $\bar{L}$ of $\mathcal{G}_{\text{full}}$ is related to the Laplacian matrix L of the network topology graph $\mathcal{G}$ as follows:

$$\bar{L} = L \otimes M, \tag{4}$$

where $\otimes$ denotes the Kronecker product, and $M = [m_{ij}] \in \{0, 1\}^{n \times n}$ is the "coupling matrix" that defines how the state variables are interconnected among themselves. That is, if $m_{\bar{i}\bar{j}} = 1$, then an edge connecting node v_j to v_i in $\mathcal{G}$ is actually coupling the state variable $x_{\bar{j}j}$ to $x_{\bar{i}i}$ in $\mathcal{G}_{\text{full}}$.

For instance, note that the "full graph" in Fig. 1c can be represented as in (3). Furthermore, if we assume that $\alpha_i = \alpha$ (yielding $A_i = A$), for $i = 1, 2, 3$, then (3) can be represented in a compact form as:

$$\dot{\boldsymbol{x}} = (I_3 \otimes A - L \otimes M)\, \boldsymbol{x}, \tag{5}$$

where I_3 is the identity matrix of order 3. Indeed, this compact notation highlights the several levels of interplay in a dynamical network, including: (i) the nodal dynamics A, (ii) the network topology L, (iii) and the coupled state variables between interconnected nodes, represented by the coupling matrix M.

Example 1 **Network of Rössler systems**

Throughout the text, the well-known Rössler system (Rössler 1976):

$$\begin{cases} \dot{x} &= -y - z \\ \dot{y} &= x + ay \\ \dot{z} &= b + z(x - c) \end{cases} \tag{6}$$

will be used as an illustration example due to its interesting observability properties. This system settles to a chaotic attractor for $(a, b, c) = (0.398, 2, 4)$.

Figure 2 illustrates how the Rössler system can be represented as a "nonlinear graph," proposed by Letellier et al. (2018), using the Jacobian matrix $D\boldsymbol{f}$ of (6):

$$D\boldsymbol{f} = \begin{bmatrix} 0 & -1 & -1 \\ 1 & a & 0 \\ z & 0 & x - c \end{bmatrix}. \tag{7}$$

[3] Two variables $(\boldsymbol{x}_i, \boldsymbol{x}_j)$ are diffusively coupled by a coupling function $\boldsymbol{g}(\boldsymbol{x}_i, \boldsymbol{x}_i)$ if $\boldsymbol{g}(\boldsymbol{x}_i, \boldsymbol{x}_j) = 0$ and $\boldsymbol{g}(\boldsymbol{x}_i, \boldsymbol{x}_j) = -\boldsymbol{g}(\boldsymbol{x}_j, \boldsymbol{x}_i)$.

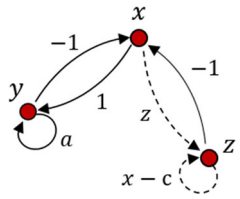

Fig. 2 Nonlinear graph of the (Jacobian matrix of the) Rössler system. Linear and nonlinear edges are represented by solid and dashed lines, respectively. This convention is a reminder that nonlinear connections are no longer constant and might vanish under specific circumstances. For instance, edges $a_{33} = x - c$ and $a_{31} = z$ vanish at $x(t) = c$ and $z(t) = 0$, respectively. Such singularities might have a huge impact on the "information flow" between two nodes interconnected by a nonlinear edge

Consider now a network of m Rössler oscillators linearly coupled by means of the variable y (Pecora and Carroll 1990; Boccaletti et al. 2002). Hence, at each node $v_i \in \mathcal{V}$, there is a system with state variables $\boldsymbol{x}_i = \begin{bmatrix} x_i & y_i & z_i \end{bmatrix}^\mathsf{T}$. The dynamical network can be represented by the following state-space model:

$$\begin{cases} \dot{x}_i &= -y_i - z_i \\ \dot{y}_i &= x_i + a_i y_i + \sum_{j=1}^m a_{ij}(y_j - y_i) \\ \dot{z}_i &= b_i + z_i(x_i - c_i) \end{cases}, \tag{8}$$

for $i = 1, \dots, m$, (a_i, b_i, c_i) are the parameters of the ith Rössler system, and $A_{\text{adj}} = \begin{bmatrix} a_{ij} \end{bmatrix}$. This is a state-space model of dimension $N = 3m$.

Coupling the Rössler oscillators directly from y to x, yields

$$\begin{cases} \dot{x}_i &= -y_i - z_i + \sum_{j=1}^m a_{ij}(y_j - x_i) \\ \dot{y}_i &= x_i + a_i y_i \\ \dot{z}_i &= b_i + z_i(x_i - c_i) \end{cases} \tag{9}$$

or undirectedly coupled by all variables (also known as "network of networks" (Chapman et al. 2014)):

$$\begin{cases} \dot{x}_i &= -y_i - z_i + \sum_{j=1}^m a_{ij}(x_j - x_i) \\ \dot{y}_i &= x_i + a_i y_i + \sum_{j=1}^m a_{ij}(y_j - y_i) \\ \dot{z}_i &= b_i + z_i(x_i - c_i) + \sum_{j=1}^m a_{ij}(z_j - z_i) \end{cases} \tag{10}$$

for $i = 1, \dots, m$.

Dynamical networks (8), (9) and (10) are illustrated as full networks in Fig. 3. Equations (8)–(10) can be represented similarly to (5), highlighting the network structure and coupling variable, as follows:

$$\dot{\boldsymbol{x}} = \boldsymbol{f}(\boldsymbol{x}) - (L \otimes M)\, \boldsymbol{x}, \tag{11}$$

where $\boldsymbol{x} = [x_1 \ y_1 \ z_1 \ \dots \ x_m \ y_m \ z_m]^\mathsf{T}$, $\boldsymbol{f} = [\boldsymbol{f}_1^\mathsf{T}(\boldsymbol{x}_1) \ \dots \ \boldsymbol{f}_m^\mathsf{T}(\boldsymbol{x}_m)]^\mathsf{T} : \mathbb{R}^N \mapsto \mathbb{R}^N$, $\boldsymbol{f}(\boldsymbol{x}_i) : \mathbb{R}^3 \mapsto \mathbb{R}^3$ is a nonlinear

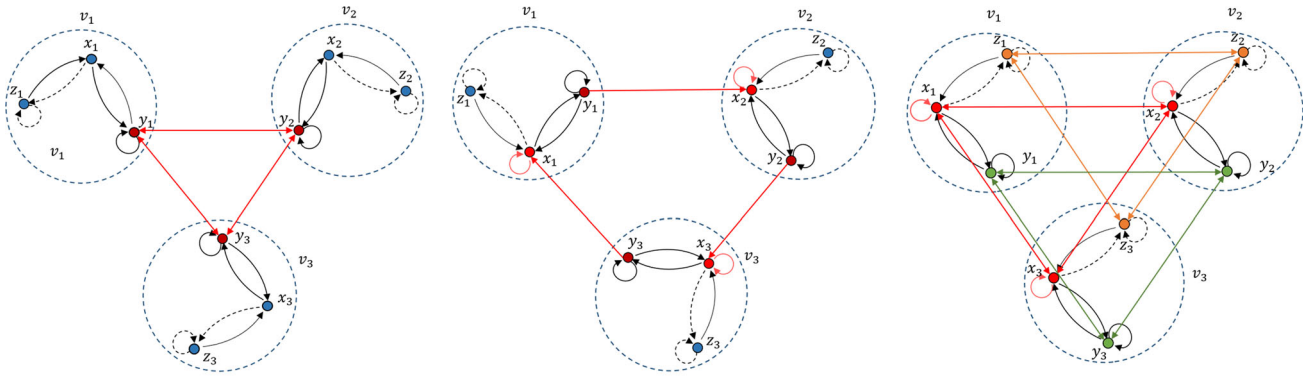

Fig. 3 Full network $\mathcal{G}_{\text{full}}$ of Rössler systems coupled **a** undirectedly by y variable (diffusive coupling), **b** directly from variable y to x, and **c** undirectedly between all respective variables. The network topology $\mathcal{G}$ is a cycle graph with $m = 3$. Self-edges are included (or have the weight modified, if already present) to the coupled vertices because of the diffusive coupling. Note that, unlike for Fig. 1, in example (**b**) $\mathcal{G}$ is not a subgraph of $\mathcal{G}_{\text{full}}$

function that describes the nodal dynamics of $\boldsymbol{x}_i$ according to (6), and the coupling matrix M is given by

$$M = \begin{bmatrix} 0\,0\,0 \\ 0\,1\,0 \\ 0\,0\,0 \end{bmatrix}, \quad \begin{bmatrix} 0\,1\,0 \\ 0\,0\,0 \\ 0\,0\,0 \end{bmatrix}, \quad \text{or} \quad \begin{bmatrix} 1\,0\,0 \\ 0\,1\,0 \\ 0\,0\,1 \end{bmatrix}, \tag{12}$$

for (8), (9) and (10), respectively. △

3 Structural Observability

We hereby address as *structural observability* to any crisp definition of observability based on a "yes-no" condition, i.e., a definition that classifies a system as either observable or not.

3.1 Linear Dynamical Systems

The classic concept of observability for linear systems was introduced by Kalman (1959). The following definition and theorem is further discussed and proven in many textbooks in linear systems theory, including the work by Chen (1999).

Definition 1 (Chen 1999, Definition 6.O1) The linear system (1) or the pair (A, C) is said to be observable if for any unknown initial state $\boldsymbol{x}(0)$, there exists a finite time $t_1 > 0$ such that the knowledge of the input $\boldsymbol{u}$ and the output $\boldsymbol{y}$ over $t \in [0, t_1]$ suffices to uniquely determine $\boldsymbol{x}(0)$. Otherwise, (1) is said to be unobservable.

Theorem 1 (Chen 1999, Theorem 6.O1) *The following statements are equivalent.*

1. *The n-dimensional pair* (A, C) *is observable.*
2. *The matrix* $W_o(t) \in \mathbb{R}^{n\times n}$

$$W_o(t) = \int_0^t e^{A^\mathsf{T}\tau} C^\mathsf{T} C e^{A\tau} d\tau \tag{13}$$

is nonsingular for any $t > t_0$.
3. *The observability matrix* $\mathcal{O} \in \mathbb{R}^{nq\times n}$

$$\mathcal{O} = \begin{bmatrix} C \\ CA \\ CA^2 \\ \vdots \\ CA^{n-1} \end{bmatrix} \tag{14}$$

has full column rank, i.e., $\operatorname{rank}(\mathcal{O}) = n$.
4. *The matrix* $\begin{bmatrix}(A - \lambda_i I)^\mathsf{T} & C^\mathsf{T}\end{bmatrix}^\mathsf{T}$ *has full column rank at every eigenvalue* λ_i *of* A, *for* $i = 1, \ldots, n$.
5. *If* $\operatorname{Re}\{\lambda_i\} < 0$, *for all* $i = 1, \ldots, n$, *then the unique solution of*

$$A^\mathsf{T} W_o + W_o A = -C^\mathsf{T} C \tag{15}$$

is positive definite, is called observability Gramian and can be expressed as

$$W_o = \int_0^\infty e^{A^\mathsf{T}\tau} C^\mathsf{T} C e^{A\tau} d\tau. \tag{16}$$

For a detailed proof, see (O'Reilly 1983; Chen 1999). We state here an interesting interpretation of the observability matrix (14). Consider the linear system (1), where the temporal evolution of $\boldsymbol{y}(t)$ is given by

$$\boldsymbol{y}(t) = Ce^{At}\boldsymbol{x}(0) + C\int_0^t e^{A(t-\tau)} B\boldsymbol{u}(\tau) d\tau + D\boldsymbol{u}(t). \tag{17}$$

Following Definition 1, since we suppose that $\boldsymbol{u}(t)$ and $\boldsymbol{y}(t)$ are known over $t \in [0, t_1]$, (17) can be rewritten as

$$\bar{\boldsymbol{y}}(t) = Ce^{At}\boldsymbol{x}(0). \tag{18}$$

where $\bar{\boldsymbol{y}}(t) := \boldsymbol{y}(t) - C\int_0^t e^{A(t-\tau)}B\boldsymbol{u}(\tau)d\tau + D\boldsymbol{u}(t)$ is a known variable. From Definition 1, system (1) is observable if $\boldsymbol{x}(0)$ can be solved from (18). Differentiating (18) successively around $t = 0$ yields

$$\begin{bmatrix} \bar{\boldsymbol{y}}(0) \\ \bar{\boldsymbol{y}}^{(1)}(0) \\ \vdots \\ \bar{\boldsymbol{y}}^{(n-1)}(0) \end{bmatrix} = \begin{bmatrix} C \\ CA \\ \vdots \\ CA^{n-1} \end{bmatrix} \boldsymbol{x}(0) \tag{19}$$
$$\tilde{\boldsymbol{y}}(0) := \mathcal{O}\boldsymbol{x}(0).$$

Equation (19) is a set of linear algebraic equations. Since $\tilde{\boldsymbol{y}}(0)$ is known, the initial state $\boldsymbol{x}(0)$ can be uniquely determined if $\tilde{\boldsymbol{y}}(0)$ lies in the column space of $\mathcal{O}$. It is straightforward to see that condition (3) of Theorem 1 is sufficient and necessary for the observability of dynamical system. Indeed, if a pair (A, C) is observable, then a solution for (19) exists, given by

$$\boldsymbol{x}(0) = \mathcal{O}^{\dagger}\tilde{\boldsymbol{y}}(0), \tag{20}$$

where $\mathcal{O}^{\dagger}$ denotes the Moore-Penrose inverse (pseudoinverse). Since $\text{rank}(\mathcal{O}) = n$, then $\mathcal{O}^{\dagger} := \left(\mathcal{O}^{\mathsf{T}}\mathcal{O}\right)^{-1}\mathcal{O}^{\mathsf{T}}$ and, therefore, solution $\boldsymbol{x}(0)$ is unique.

Remark 1 Computation of (20) is not feasible for practical applications since it requires differentiation of $\bar{\boldsymbol{y}}(t)$, which amplifies high-frequency noise in measurements. Nevertheless, proving that $\text{rank}(\mathcal{O}) = n$ guarantees that $\boldsymbol{x}(t_0)$ can be uniquely determined and is also a sufficient and necessary condition for existence of stable state observers. Moreover, the observability matrix is also related to subspace identification methods (Overschee and De Moor 1996; Haber and Verhaegen 2014).

Note that, Definition 1 only classifies the pair (A, C) as observable or unobservable. Thus, we refer to Theorem 1 as a *structural observability* property. This *crisp* classification is due to the observability property being based on a rank condition of (14). Consequently, the observability property is a discontinuous function of the system parameters. Hence, a small change in the parameter space of (1) can move a dynamical system from unobservable to observable, and vice versa.

Suppose that matrix $\mathcal{O}^{\mathsf{T}}\mathcal{O}$ is nonsingular, but *ill-conditioned*. For practical purposes, this means that the computation of its inverse is prone to large numerical errors, leading to large errors in the solution of (20). One might argue that in this case, a pair (A, C) is *almost unobservable*—or rather unobservable for practical purposes—and, therefore, the structural observability property of Theorem 1 is not suitable for certain applications due to its sensitivity to an ill-conditioned matrix (Friedland 1975). This problem is further explored in Sect. 4.

3.2 Nonlinear Dynamical Systems

Several generalizations to observability of nonlinear systems have been proposed in the literature (Hermann and Krener 1977; Sontag 1991; Zabczyk 1995; Letellier and Aguirre 2009; Zhirabok and Shumsky 2012; Mesbahi et al. 2019). This work follows the definition of *local weak observability*, grounded on differential geometry, established by Hermann and Krener (1977).

Consider the nonlinear system (2), or the pair $\{\boldsymbol{f}, \boldsymbol{h}\}$. Let the flow map $\boldsymbol{\Phi}_t(\boldsymbol{x}(t_0)) : \mathcal{M} \mapsto \mathcal{M}$ be the solution of (2), which defines the trajectory from a initial state $\boldsymbol{x}(t_0)$ to a final state $\boldsymbol{x}(t_0 + t)$, given by

$$\boldsymbol{\Phi}_t(\boldsymbol{x}(t_0)) := \boldsymbol{x}(t_0 + t) = \boldsymbol{x}(t_0) + \int_{t_0}^{t_0+t} \boldsymbol{f}(\boldsymbol{x}(\tau))\mathrm{d}\tau. \tag{21}$$

From Definition 1, the concept of observability can be generalized to nonlinear systems (2) by determining whether or not an initial state $\boldsymbol{x}(t_0)$ can be uniquely reconstructed from the image of the composition map $\boldsymbol{h} \circ \boldsymbol{\Phi}_t$. This is formally defined as follows (Hermann and Krener 1977; Mesbahi et al. 2019).

Definition 2 The nonlinear system (2), or the pair $\{\boldsymbol{f}, \boldsymbol{h}\}$, is

- **locally observable at** $\boldsymbol{x}_0$ if there exists a neighborhood $\mathcal{U} \subseteq \mathcal{M}$ of $\boldsymbol{x}_0$ such that for every state $\boldsymbol{x}_0 \neq \boldsymbol{x}_1 \in \mathcal{U}$, $\boldsymbol{h} \circ \boldsymbol{\Phi}_t(\boldsymbol{x}_0) \neq \boldsymbol{h} \circ \boldsymbol{\Phi}_t(\boldsymbol{x}_1)$ for some finite $t > t_0$;
- **locally observable** if it is locally observable at every $\boldsymbol{x}_0 \in \mathcal{M}$;
- and **observable** if its locally observable and the neighborhood $\mathcal{U}$ can be taken as $\mathcal{M}$.

Otherwise, $\{\boldsymbol{f}, \boldsymbol{h}\}$ is said to be locally unobservable at $\boldsymbol{x}_0$.

An advantage of the local observability definition is that it can be verified through a simple algebraic test as follows.

Theorem 2 *Let the nonlinear system (2), or the pair* $\{\boldsymbol{f}, \boldsymbol{h}\}$ *be of class* C^s, $s \geq 1$. *The pair* $\{\boldsymbol{f}, \boldsymbol{h}\}$ *is locally observable at* $\boldsymbol{x}_0$ *if the observability matrix*

$$\mathcal{O}(\boldsymbol{x}_0) = \frac{\partial}{\partial \boldsymbol{x}} \begin{bmatrix} \mathcal{L}_f^0 \boldsymbol{h}(\boldsymbol{x}) \\ \vdots \\ \mathcal{L}_f^{s-1} \boldsymbol{h}(\boldsymbol{x}) \end{bmatrix}_{\boldsymbol{x}=\boldsymbol{x}_0}, \tag{22}$$

is full rank, i.e., $\text{rank}(\mathcal{O}(\boldsymbol{x}_0)) = n$, *where* $\mathcal{L}_{\boldsymbol{f}}^{j}\boldsymbol{h}(\boldsymbol{x}_0) := \nabla \boldsymbol{h} \cdot \boldsymbol{f}$ *is the* j*-th Lie derivative of* $\boldsymbol{h}$ *along the vector field* $\boldsymbol{f}$ *at* $\boldsymbol{x} = \boldsymbol{x}_0$.

Proof (Klaus and Reinschke 1999) From Definition 2, $\{\boldsymbol{f}, \boldsymbol{h}\}$ is observable if the map

$$\boldsymbol{\Psi}_h(\boldsymbol{x}) : \boldsymbol{x} \mapsto \left[\boldsymbol{y}^{\mathsf{T}} \left[\boldsymbol{y}^{(1)}\right]^{\mathsf{T}} \ \ldots \ \left[\boldsymbol{y}^{(s-1)}\right]^{\mathsf{T}}\right]^{\mathsf{T}} \tag{23}$$

is invertible (injective) for a given $s \geq 1$—in other words, if it is possible to uniquely determine $\boldsymbol{x}$ from $\boldsymbol{y}$ (and its successive derivatives). The inverse function theorem provides a *sufficient condition* for local invertibility of general nonlinear maps: $\boldsymbol{\Psi}_h(\boldsymbol{x})$ is locally invertible at $\boldsymbol{x}_0$ if its Jacobian matrix has full rank, i.e.,

$$\text{rank}\left(\frac{\partial \boldsymbol{\Psi}_h(\boldsymbol{x})}{\partial \boldsymbol{x}}\right)\Bigg|_{\boldsymbol{x}=\boldsymbol{x}_0} = n. \tag{24}$$

Substituting (2) in (23), yields the nonlinear map

$$\boldsymbol{\Psi}_h(\boldsymbol{x}) := \begin{bmatrix} \boldsymbol{y} \\ \boldsymbol{y}^{(1)} \\ \vdots \\ \boldsymbol{y}^{(s-1)} \end{bmatrix} = \begin{bmatrix} \boldsymbol{h}(\boldsymbol{x}) \\ \frac{\mathrm{d}\boldsymbol{h}(\boldsymbol{x})}{\mathrm{d}t} \\ \vdots \\ \frac{\mathrm{d}^{s-1}\boldsymbol{h}(\boldsymbol{x})}{\mathrm{d}t^{s-1}} \end{bmatrix} = \begin{bmatrix} \mathcal{L}_{\boldsymbol{f}}^{0}\boldsymbol{h}(\boldsymbol{x}) \\ \mathcal{L}_{\boldsymbol{f}}^{1}\boldsymbol{h}(\boldsymbol{x}) \\ \vdots \\ \mathcal{L}_{\boldsymbol{f}}^{s-1}\boldsymbol{h}(\boldsymbol{x}) \end{bmatrix}, \tag{25}$$

where higher-order Lie derivatives are defined as

$$\mathcal{L}_{\boldsymbol{f}}^{j}\boldsymbol{h}(\boldsymbol{x}) := \frac{\partial \mathcal{L}_{\boldsymbol{f}}^{j-1}\boldsymbol{h}(\boldsymbol{x})}{\partial \boldsymbol{x}} \boldsymbol{f}(\boldsymbol{x}), \tag{26}$$

for $\mathcal{L}_{\boldsymbol{f}}^{0}\boldsymbol{h}(\boldsymbol{x}) := \boldsymbol{h}(\boldsymbol{x})$.

It follows that the Jacobian matrix of $\boldsymbol{\Psi}_h(\boldsymbol{x})$ is equivalent to $\mathcal{O}(\boldsymbol{x})$, and hence, condition (24) implies local invertibility (and observability) at $\boldsymbol{x}_0$. □

Remark 2 It follows that (22) reduces to (14) if $\boldsymbol{f}$ and $\boldsymbol{h}$ are linear functions.

Remark 3 In the context of single measurement ($q = 1$), the nonlinear observability matrix (22) is full rank only if $s \geq n$. Theoretically, however, the necessary number s of Lie derivatives so that the nonlinear system is observable depends on $\{\boldsymbol{f}, \boldsymbol{h}\}$ and can even tend to infinity (Zabczyk 1995; Mesbahi et al. 2019).

The discussion in Sect. 3.1 regarding this crisp classification of observability and the effects of ill-conditioning of $\mathcal{O}$ also holds for the nonlinear case. Naturally, computational burden is aggravated for the nonlinear case, since computation of (22) is more computationally intensive than (14).

3.2.1 Observability and Embedding Theory

A relation between observability and embedding theory follows naturally from the proof of Theorem 2 (Letellier et al. 2005). If $h : \mathbb{R}^n \to \mathbb{R}^1$ and $y \in \mathbb{R}^1$ (single output), then the pair $\{\boldsymbol{f}, h\}$ is locally observable if the Jacobian matrix of the map $\boldsymbol{\Psi}_h$ is locally nonsingular. In this case, (22) is the Jacobian matrix of the map $\boldsymbol{\Psi}_h$ between the original state-space and the n-dimensional differential embedding space (Letellier et al. 2005).[4] If $\boldsymbol{\Psi}_h$ is nonsingular for all $\boldsymbol{x}$, then there is a global diffeomorphism and the pair $\{\boldsymbol{f}, h\}$ is fully and globally observable.

Example 2 **Structural observability.**

Consider Rössler system (6). If $h(\boldsymbol{x}) = y$ (the recorded variable is the y variable of the Rössler system), then the observability matrix $\mathcal{O}_y(\boldsymbol{x})$ (or the Jacobian matrix of the map $\boldsymbol{\Psi}_y^3 : \boldsymbol{x} \mapsto \left[y \ \ \dot{y} \ \ \ddot{y}\right]$) is

$$\frac{\partial \boldsymbol{\Psi}_y^3}{\partial \boldsymbol{x}} \equiv \mathcal{O}_y(\boldsymbol{x}) = \begin{bmatrix} 0 & 1 & 0 \\ 1 & a & 0 \\ a & a^2 - 1 & -1 \end{bmatrix}. \tag{27}$$

Since $\mathcal{O}_y(\boldsymbol{x})$ is constant and nonsingular (implying full rank) for all $\boldsymbol{x} \in \mathbb{R}^n$, the Rössler system is fully (globally) observable from the y variable.

If $h(\boldsymbol{x}) = z$, then the observability matrix $\mathcal{O}_z(\boldsymbol{x})$ (or the Jacobian matrix of the map $\boldsymbol{\Psi}_z^3 : \boldsymbol{x} \mapsto \left[z \ \ \dot{z} \ \ \ddot{z}\right]$) is

$$\frac{\partial \boldsymbol{\Psi}_z^3}{\partial \boldsymbol{x}} \equiv \mathcal{O}_z(\boldsymbol{x}) = \begin{bmatrix} 0 & 0 & 1 \\ z & 0 & x - c \\ b + 2z(x - c) & -z & (x - c)^2 - y - 2z \end{bmatrix}. \tag{28}$$

Since $\mathcal{O}_z(\boldsymbol{x})$ is not constant, we refer to Theorem 2. Note that, $\mathcal{O}_z(\boldsymbol{x})$ is singular for $z = 0$, since $\det(\mathcal{O}_z(\boldsymbol{x})) = -z^2$. Thus, considering the definition of structural observability, the Rössler system is unobservable for $z = 0$ and observable for $z \in \mathbb{R}\backslash\{0\}$.

This raises the following question: how good is the trajectory reconstruction from measurements on z in the vicinity of $z = 0$? This question is further explored with the definition of dynamical observability. △

4 Dynamical Observability

As detailed in Sect. 3, the structural classification of observability faces several practical problems, such as the feasibility of reconstructing a dynamical system trajectory from a set of

[4] The relation between the observability matrix and the Jacobian matrix of map $\boldsymbol{\Psi}_h$ was investigated for multivariate embedding ($\boldsymbol{h} : \mathbb{R}^n \mapsto \mathbb{R}^q$) in (Aguirre and Letellier 2005).

output signals whose observability matrix is ill-conditioned (sensitive to small changes). If one has access to different sets of output signals for a given dynamical system, it is relevant, for practical purposes, to classify a system not only as observable or not, but also to establish a continuous quantification of observability levels conveyed by each available set of output signals. In this way, one can distinct observable systems between conditions of "poor" and "rich" observability, which directly affect the reconstruction quality of the dynamical system trajectory. Metrics that quantify observability in a continuous manner, rather than discrete, are referred in this work as *dynamical observability* coefficients (Aguirre et al. 2018).

4.1 Linear Dynamical Systems

As the problem of investigating dynamical observability seems to be related with the conditioning of matrix $\mathcal{O}$, Friedland (1975) proposed the *condition number* as an alternative:

$$\kappa(A) = \left\|A^{-1}\right\| \|A\| = \frac{\sigma_1(A)}{\sigma_n(A)}, \tag{29}$$

where we have used the ℓ_2-norm, and $\sigma_1 \geq \sigma_2 \geq \ldots \geq \sigma_n$ are the singular values of a square matrix A. As $\kappa(A)$ increases, the numerical condition of A degrades.

Friedland (1975) adapted the conditioning number for a more intuitive quantification of observability as follows.

Definition 3 The "coefficient of observability" of a pair (A, C) is defined as

$$\delta := \left|\frac{\lambda_{\min}(F)}{\lambda_{\max}(F)}\right|. \tag{30}$$

where $0 \leq \delta \leq 1$, $F = \mathcal{O}^{\mathsf{T}}\mathcal{O}$ or $F = W_o$, and $\lambda_{\min}$ and $\lambda_{\max}$ refer to the minimum and maximum eigenvalues[5] of F. If $\lambda_{\max}(F) = 0$, then necessarily $\lambda_{\min}(F) = 0$ and the dimension of the observable space is zero by definition.

Larger values of δ indicate that (A, C) is more observable. Thus, even when $\mathcal{O}$ is full rank, a small δ points to *poor observability*. If $\delta = 0$, then (A, C) is not observable. The use of observability coefficients allows one to decide if a given set of output signals (e.g., $\boldsymbol{y}_1 = C_1\boldsymbol{x}$) conveys more or less observability to the dynamical system (1) than another set of output signals (e.g., $\boldsymbol{y}_2 = C_2\boldsymbol{x}$). Thus, if both pairs (A, C_1) and (A, C_2) are observable according to Theorem 1, one can use Definition 3 to distinguish between conditions of "poor" and "rich" observability, which directly affects the reconstruction quality of this dynamical system trajectory (Montanari and Aguirre 2019).

[5] Since F is symmetric, its singular values are equal to the absolute values of its eigenvalues.

Remark 4 Although the structural observability definition is invariant under similarity transformations (Chen 1999, Theorem 6.02), the coefficient of dynamical observability δ is sensitive to similarity transformations (Aguirre 1995).

Remark 5 Coefficient δ usually increases with the dimension q: typically more outputs increase the quality of observability. However, this is not always true for some networks of oscillators (Montanari and Aguirre 2019).

Definition 3 is found in several works in the literature based on the conditioning number of the observability matrix (Friedland 1975; Aguirre and Letellier 2005; Whalen et al. 2015; Wang et al. 2017; Aguirre et al. 2018; Montanari and Aguirre 2019; Luan and Tsvetkov 2019). Nevertheless, it is worth mentioning that other coefficients of dynamical observability have been proposed in the literature based on the observability Gramian (Johnson 1969; Pasqualetti et al. 2013; Summers et al. 2016):

- the trace of the Gramian $\mathrm{tr}(W_o)$, related to the average observation energy in all directions of the observable subspace;
- the determinant of the Gramian $\det(W_o)$, a volumetric measure of the set of spaces which can be observed within one unit of energy;
- and the smallest eigenvalue of the Gramian $\lambda_{\min}(W_o)$, a worst-case metric related to the amount of energy required to observe the most difficult state.

It is not yet clear in the literature the distinction between coefficients of observability based on the observability Gramian and the observability matrix.[6] For instance, Sun and Motter (2013) show that a given continuous-time dynamical system might have an ill-conditioned observability Gramian and a well-conditioned observability matrix. A work in progress, however, shows that these coefficients have different interpretations and therefore different impacts on the quality of state reconstruction depending whether the system is poorly observable due to the ill-conditioning of the observability Gramian and/or the observability matrix (Montanari 2019).

4.2 Nonlinear Dynamical Systems

Definition 3 was extended to nonlinear dynamical systems by Letellier et al. (1998); Letellier and Aguirre (2002).

[6] Especially in the context of continuous-time systems. In the discrete-time case, the definitions of the observability matrix and Gramian are equivalent.

Definition 4 The "local coefficient of observability" at $\boldsymbol{x}_0$ of a pair $\{\boldsymbol{f}, \boldsymbol{h}\}$ is defined as

$$\delta(\boldsymbol{x}_0) := \left| \frac{\lambda_{\min}(\mathcal{O}^{\mathsf{T}}(\boldsymbol{x}_0) \cdot \mathcal{O}(\boldsymbol{x}_0))}{\lambda_{\max}(\mathcal{O}^{\mathsf{T}}(\boldsymbol{x}_0) \cdot \mathcal{O}(\boldsymbol{x}_0))} \right|, \tag{31}$$

where $0 \leq \delta(\boldsymbol{x}_0) \leq 1$. The "global coefficient of observability" of $\{\boldsymbol{f}, \boldsymbol{h}\}$ is the average along a trajectory $\boldsymbol{\Phi}_{t_1}(\boldsymbol{x}(t_0))$, for $t \in [t_0, t_1]$:

$$\delta = \frac{1}{t_1 - t_0} \int_{t_0}^{t_1} \delta_y(\boldsymbol{x}(t)) \mathrm{d}t. \tag{32}$$

The coefficient in (32) is not normalized. Hence, it is not meaningful to compare the coefficient of observability of variables (or sets of output signals) for *different* systems. It must be noted that the comparison is relative (Aguirre et al. 2008).

Example 3 **Dynamical observability.**

Consider Rössler system (6) and the observability matrix $\mathcal{O}_y(\boldsymbol{x})$ built considering variable y as the measured (recorded) signal (see (27)). Since $\mathcal{O}_y$ is constant over the entire state space, there is a global diffeomorphism between original and reconstructed spaces. Computing (31) yields $\delta_y = 0.133$.

On the other hand, consider $\mathcal{O}_z(\boldsymbol{x})$ in (28). As explained in Example 2, since $\det(\mathcal{O}_z(\boldsymbol{x})) = -z^2$, the system is not observable at $z = 0$ and, from a dynamical observability point of view, it is poorly observable in the vicinity of the plane $z = 0$. For instance, for $z = 0.3$, using (31) yields $\delta_z(z = 0.3) = 1.32 \cdot 10^{-6}$. However, equation (31) only provides a *local* quantification of the variable z observability. For a more *global* quantification, we compute the average (32) over the entire chaotic attractor, which yields $\delta_z = 0.006$—indicating, nonetheless, the poor observability of z when compared to y.

For the Rössler system with $(a, b, c) = (0.398, 2, 4)$, the following values were computed using (32): $\delta_x = 0.022$, $\delta_y = 0.133$, $\delta_z = 0.006$. Since $\delta_y > \delta_x > \delta_z$, it is stated that the *observability rank* of the recorded variables is $y \triangleright x \triangleright z$ (Letellier and Aguirre 2002). △

Examples 2 and 3 show that the loss of *local observability* is intrinsically related to the local singularities that $\boldsymbol{\Psi}_h$ may have, which are a consequence of nonlinearities. The following remark holds generally, though.

Remark 6 According to Takens' theorem (Takens 1981), assuming that $\{\boldsymbol{f}, h\}$ is structurally observable, if the dimension of the reconstructed space is increased, that is $\boldsymbol{\Psi}_h : \boldsymbol{x} \mapsto \left[y \;\; y^{(1)} \;\; \ldots \;\; y^{(s-1)}\right]^{\mathsf{T}}$, with $s > n$ usually, then any singularities of $\boldsymbol{\Psi}_h$ may vanish and the pair $\{\boldsymbol{f}, h\}$ gradually becomes more dynamically observable (Letellier et al. 2005).

5 Topological Observability

Sections 3 and 4 approached the study of observability from a system theory point of view. However, the developed methods are not particularly efficient for high-dimensional dynamical systems such as networks. Indeed, even if the full network dynamics were known, to find a set of sensor nodes that render a full network observable would require a brute force computation of $\mathcal{O}$ over $(2^N - 1)$ distinct combinations (Liu et al. 2011)—which is not feasible at all. This process would be even more demanding if computation of eigenvalues in (30) or Lie derivatives in (22) were involved.

Faced with these challenges, a possible strategy to study the observability of a network system is to investigate it from a graph approach, which we refer to as *topological observability*. In this case, the topological observability is usually assessed solely from the network topology graph, although some works argue that the results are more representative when the topological observability is assessed from the full network graph (Cowan et al. 2012; Leitold et al. 2017; Aguirre et al. 2018), as discussed in Sect. 2.2.

Most studies developed over this idea follow the pioneer line of work of Liu et al. (2011), grounded on the structural observability definition of Lin (1974).

5.1 Linear Dynamical Systems

Lin (1974) proposed a novel concept of structural controllability for linear systems, which was later extended to observability (Willems 1986).

Definition 5 (Li et al. 2019, Definition 1) A matrix $\bar{A} \in \{0, \star\}^{n \times n}$ is called a structured matrix if $A = [a_{ij}]$ is either a fixed zero entry or an independent free parameter, denoted by a $\star$. A matrix $\tilde{A}$ is a numerical realization of A if a real number is assigned to all free parameters of A.

Definition 6 The structured pair (A, C) is structurally observable if and only if there exists some numerical realization $(\tilde{A}, \tilde{C})$ that is observable.

Remark 7 Definition 5 is grounded on the assumption that, in real applications, the true entries of (A, B, C, D) are usually uncertain, while zero entries are somewhat guaranteed (Lin 1974). Thus, if a system is structurally observable, then it is observable for a wide range of parameters except for a *proper algebraic variety* in the parameter space which renders it unobservable (Liu et al. 2011).

Remark 8 A possible interpretation to Definition 5 based on graph theory is that two pairs (A_0, C_0) and (A_1, C_1) are of the same structure if their corresponding graphs share the same structure, i.e., the same set of nodes $\mathcal{V}$ and edges $\mathcal{E}$, although the edge weights do not need to share the same values—provided that they are different from zero.

Remark 9 Note that, Lin's definition of structural observability is structural in two senses: (i) it is a crisp definition, as detailed in Sect. 3; and (ii) it is independent of the specific entries of (A, B, C, D)—relying only on the fact that zero entries are specifically known. "Structural observability (controllability) in Lin's sense" (Definition 6) is only a *necessary* condition for "structural observability (controllability) in Kalman's sense" (Definition 1).

Lin (1974) provided an insightful analysis to determine the structural controllability of a system by drawing a graph associated with the pair (A, B). Lin states that a pair (A, B) is uncontrollable if its corresponding graph has *non-accessible* nodes from the driver nodes. In this section, since our main concern is with observability, we present and detail an extension of Lin's work for determination of structural observability following the *duality theorem* (Chen 1999, Theorem 6.5) as presented by Aguirre et al. (2018). Thus, (A, C) is structurally observable if and only if $(A^\mathsf{T}, C^\mathsf{T})$ is structurally controllable.

Let a linear system (1), or a pair (A, C), be expressed as structured matrices

$$A = \begin{bmatrix} \star & \star & 0 \\ \star & \star & 0 \\ \star & \star & \star \end{bmatrix}, \quad C = \begin{bmatrix} 0 & 0 & \star \end{bmatrix}. \tag{33}$$

Following nomenclature in Sect. 2.2, pair (A, C) can be represented by a graph $\mathcal{G}(A, C) = \{\mathcal{X} \cup \mathcal{S}, \mathcal{E}_\mathcal{X} \cup \mathcal{E}_\mathcal{S}\}$, where the system state variables $\boldsymbol{x}$ are designated as a *set of state nodes* $\mathcal{X} = \{x_1, \ldots, x_n\}$ and the output variables $\boldsymbol{y}$ are designated to a *set of sensor nodes* $\mathcal{S} = \{y_1, \ldots, y_q\}$. An edge (x_i, x_j) (directed arrow from x_j to x_i) is an element of $\mathcal{E}_\mathcal{X}$ if a_{ij} is a free parameter entry of structured matrix A, and an edge (y_i, x_j) is an element of $\mathcal{E}_\mathcal{S}$ if c_{ij} is a free parameter entry of structured matrix C. Hence, a graph of (33) can be drawn from

$$A_{\text{adj}} = \begin{bmatrix} A \\ C \end{bmatrix} = \begin{bmatrix} \star & \star & 0 \\ \star & \star & 0 \\ \star & \star & \star \\ 0 & 0 & \star \end{bmatrix} \tag{34}$$

as shown in Fig. 4. A necessary condition for a pair (A, C) to be structurally observable is the existence of a direct path from all vertices in $\mathcal{X}$ to any sensor node in $\mathcal{S}$. Since from all nodes $\mathcal{X} = \{x_1, x_2, x_3\}$, it is possible to reach y_1, we note that the graph in Fig. 4 is structurally observable according to Lin's definition.

Remark 10 If A or C are transposed, the directions of the corresponding edges (that is, the direction of the arrows) in $\mathcal{G}(A, C)$ should be reversed.

Fig. 4 Graph representation of (34)

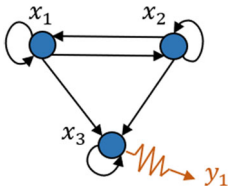

The following theorem derives from this graph approach to structural observability.

Theorem 3 (Lin 1974, See equivalent theorem and proof for controllability) *The pair (A, C) is structurally observable by Definition 6 if and only if, in the respective graph $\mathcal{G}(A^\mathsf{T}, C^\mathsf{T})$, every state $x_i \in \mathcal{X}$ can be reached by a path from some output $y_i \in \mathcal{S}$, and there are no dilations.*[7]

5.1.1 Maximum Matching Algorithm

Grounded on the structural and topological definition of controllability proposed by Lin (1974), Liu et al. (2011) presented a pioneering work for controllability of *complex networks*.[8] The main goal is twofold: (i) to identify the *minimum set of driver nodes* $\mathcal{D} = \{u_1, \ldots, u_p\}$, i.e., input signals $\boldsymbol{u}$, which can steer a (linear) network system entire state; and (ii) to understand the relations between controllability and the complex network (topological) properties.

Liu et al. (2011) argued that other pioneering works on controllability of network systems, e.g., (Tanner 2004; Lombardi and Hörnquist 2007; Rahmani et al. 2009), are based on a weak assumption that, in a network system, the topology and nodal dynamics are entirely known. This assumption allowed previous works to explore the spectral graph properties of a network, such as the spectrum of the Laplacian matrix (Rahmani et al. 2009). However, even in the face of recent developments in modeling of complex networks, the accurate estimation of edge weights is not quite realistic yet. Indeed, in the case of biological or social networks, not even the nodal dynamics are fully known.

Thus, in order to study controllability of complex networks, Liu et al. (2011) turned to the topological and structural controllability definition of Lin (1974) since: (i) it has a convenient interpretation grounded on a theoretical graph approach, which is very useful when the network topology can be established; and (ii) following Remark 7, Lin's structural controllability is not sensitive to parameter fluctuations, also a convenient feature since parameter estimation is often unreliable in large network systems.

[7] A digraph $\mathcal{G}(\mathcal{A}^\mathsf{T}, \mathcal{C}^\mathsf{T})$ contains a dilation if and only if there is a subset of nodes $\mathcal{V}' \subseteq \mathcal{X}$ such that $|T(\mathcal{V}')| < \mathcal{V}'$, where $T(\mathcal{V}')$ is the set of all nodes $v_i \in \mathcal{X} \cup \mathcal{S}$ with the property that there is a direct edge from v_i to a node in $\mathcal{V}'$. Note that, in the discussed example of Fig. 4, since every node has a self-edge, $\mathcal{G}(A^\mathsf{T}, C^\mathsf{T})$ has no dilations.

[8] Although the main focus of this work is on observability, the review of Liu et al. (2011)'s proposal for controllability is still relevant due to duality.

Indeed, Liu et al. (2011) show that Lin's structural controllability problem maps into an equivalent graph problem where one can gain full control over a directed network[9] $\mathcal{G}(A, B)$ if and only if each unmatched node is directly connected to a driver node, and there are direct paths from any input signal to all matched nodes. A *matching* is formally defined as:

Definition 7 (Liu et al. 2011, Definition 8 of Supplementary Information) An edge subset $\mathcal{E}_M$ is a matching if no two edges of $\mathcal{E}_M$ share a common starting node or a common ending node. A node is matched if it is an ending node of an edge in the matching. Otherwise, it is unmatched.

This leads to the following theorem.

Theorem 4 (Liu et al. 2011, Theorem 2 of Supplementary Information) *The minimum number of driver nodes* n_{D} *needed to render* $\mathcal{G}(A, B)$*, or the pair* (A, B)*, controllable, is defined by*

$$n_{\mathrm{D}} = \max\{m - |\mathcal{E}_M|, 1\} \tag{35}$$

where m *is the number of nodes in* $\mathcal{G}(A, B)$*. If there is a perfect matching in* $\mathcal{G}(A, B)$*,* $n_{\mathrm{D}} = 1$ *(i.e.,* $|\mathcal{D}| = 1$*). Otherwise,* n_{D} *equals the number of unmatched nodes with respective to any maximum matchings (i.e.,* $\mathcal{D}$ *is composed by the unmatched nodes).*

Remark 11 Adding more edges to $\mathcal{G}(A, B)$ will never weaken a system structural controllability by Definition 6, which is not necessarily true for Definition 1. This feature makes Theorem 4 meaningful in dealing with missing links in network topology modeling (Liu et al. 2011).

Remark 12 Differently from a brute force search for a minimum $\mathcal{D}$, which is of order $\mathcal{O}(2^N)$, the maximum matching algorithm allows $\mathcal{D}$ to be identified with at most $\mathcal{O}(\sqrt{m}|\mathcal{E}|)$ steps (Liu et al. 2011)—a highly scalable algorithm to solve the minimum driver (sensor) placement problem.

From these results, Liu et al. (2011) reached several conclusions on the controllability of complex networks. The most interesting ones are: (i) controlling heterogeneous and sparse networks is harder than controlling homogeneous and dense ones; and (ii) the counter-intuitive notion that driver nodes tend to avoid high-degree nodes. Some other conclusions, such as the correlation between the n_{D} and the network degree distribution are arguable considering the applied methodology and assumptions (Cowan et al. 2012). Section 6 criticizes and discusses the main results derived from this framework.

[9] Definition of $\mathcal{G}(A, B)$ is analogous to that of $\mathcal{G}(A, C)$, where $\mathcal{G}(A, B)$ is the corresponding graph of pair (A, B).

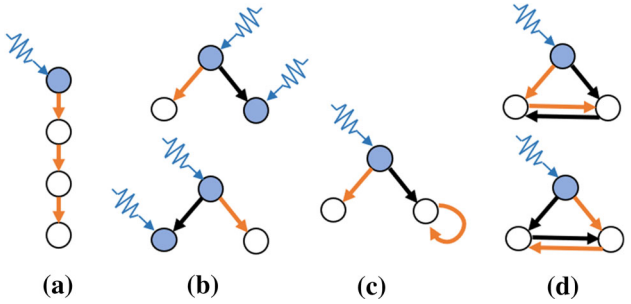

Fig. 5 Examples of maximum matching in simple networks. Set $\mathcal{E}_M$ is composed of orange edges. Unmatched and matched nodes are represented, respectively, in blue and white colors. To render the graph structurally controllable, all unmatched nodes must receive an input signal. **a** In a direct path, a network is controllable from the top node. **b** In this directed star, there are two sets $\mathcal{E}_M$ with the same minimum cardinality, thus the network is controllable for two different configurations of driver placement. **c** The addition of a self-edge removes the necessity for an additional driver node in the same network topology of (**b**). **d** The addition of a bidirectional edge has the same effect of (**c**)

Figure 5 illustrates, with some simple network examples, the available choices of $\mathcal{D}$ that render a network structurally controllable in Lin's sense via the maximum matching algorithm. This technique is readily available for use in the MATLAB-based "NOCAD" toolbox (Leitold et al. 2019).

5.2 Nonlinear Dynamical Systems

In a later work, Liu et al. (2013) proposed a means to determine the topological observability of complex networks in the context of nonlinear polynomial networks (e.g., chemical reactions). The work is also grounded on Lin's definition of observability and motivation is similar to the one stated in Sect. 5.1.1, whereas the main goal of Liu et al. (2013) is to determine the *minimum set of sensor nodes* $\mathcal{S} = \{y_1, \ldots, y_q\}$ which can render the system topologically observable.

Entitled *graph approach* (GA), Liu et al. (2013) proposed a procedure to guarantee the *topological observability* of a network:

1. draw an "inference diagram," a nonlinear graph $\mathcal{G}$, from (2) according to Sect. 2.2;[10]
2. transpose the adjacency matrix of $\mathcal{G}$ (i.e., invert the edge directions);
3. decompose $\mathcal{G}$ in *strongly connected components* (SCCs) (see "Appendix A");
4. determine the *root SCCs* (i.e., a SCC with no incoming edges);

[10] Note that, this inference diagram $\mathcal{G}$ drawn from (2) does not distinguish between linear (solid) and nonlinear (dashed) interconnections. The problem of singularities and vanishing nonlinear interconnections is explored by Letellier et al. (2018), and further illustrated in Example 4.

5. place a sensor node y_i in at least one node of each root SCC.

Remark 13 If no nodes of a root SCC are observed, the network is unobservable, because one or more columns of $\mathcal{O}(\boldsymbol{x})$ in (22) are composed of only zero entries and $\text{rank}(\mathcal{O}(\boldsymbol{x})) < n$. A more physical interpretation is that if there is no path from a given node to a sensor node (which always happens if no node of a root SCC is a sensor), then the information from this state cannot be inferred from any existing sensor nodes (Liu et al. 2013).

Remark 14 The procedure is only a *necessary condition* for observability of nonlinear polynomial systems. If all sensor nodes selected from GA are measured, then $\mathcal{O}(\boldsymbol{x})$ has no zero columns (Liu et al. 2013). Nevertheless, there is no guarantee that $\mathcal{O}(\boldsymbol{x})$ columns are linearly independent, i.e., that $\mathcal{O}(\boldsymbol{x})$ is full rank in the sense of Theorem 2.

Following Remark 14, based on an empirical analysis of multiple randomly generated chemical reactions, Liu et al. (2013) argue that the probability of correlation among the columns of $\mathcal{O}(\boldsymbol{x})$ is rather small, if not zero, due to the "complicated polynomials" entries of $\mathcal{O}(\boldsymbol{x})$. This is analogous to Remark 7 on topological observability, where it is said that the proper algebraic variety of the parameter space that renders the system unobservable is comparatively small. However, the presence of symmetries in a dynamical network can render the system unobservable (Whalen et al. 2015), leading GA to underestimate $\mathcal{S}$. This is addressed by Liu et al. (2013) when comparing the lower bound of $\mathcal{S}$ for topological observability provided by GA to the one provided by the maximum matching algorithm.

It must be mentioned that, although the probability that two columns of $\mathcal{O}(\boldsymbol{x})$ are (exactly) linearly dependent is rather small, the columns of $\mathcal{O}(\boldsymbol{x})$ might be *almost linearly dependent* nonetheless—leading to a rather small coefficient of (dynamical) observability δ. Indeed, since the GA method is based on a structural classification of observability, it cannot identify the *best* sensor placement inside a root SCC, only which sets of sensor nodes are able to render the network topologically observable.

Example 4 **Topological observability.**

We illustrate a potential failure of the GA method to classify the topological observability of a polynomial nonlinear system, the Rössler system (Letellier et al. 2018).

As detailed in Sect. 2.2, let the Rössler system be represented by a nonlinear graph (see Fig. 2). Clearly, if z tends to 0 in (6), then the nonlinear edge connecting x to z vanishes. Figure 6 represents the root SCC of a Rössler system graph when the nonlinear edge is still present and after vanishing. Following GA method, in Fig. 6a, any state (x, y or z) could be chosen as a sensor node in order to render the network topologically observable. However, if $z = 0$ one edge vanishes and z is no longer part of the root SCC. Hence, only the x and y variables could be chosen as sensor nodes in order to render the network topologically observability.

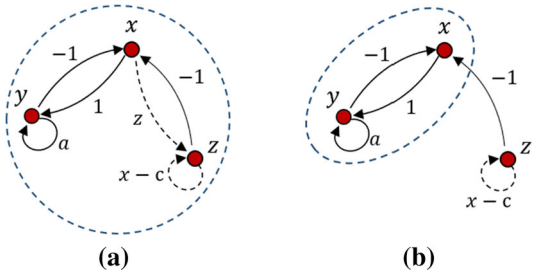

Fig. 6 Root SCC (dashed circle) of a Rössler system graph. **a** All edges are nonzero. **b** For $z = 0$, the nonlinear edge vanishes

This counter-example shows the importance of considering the singularity effects of nonlinear systems when determining the potential root SCC, especially when the system operates in the vicinity of this point of singularity. Indeed, the "vanishing" of the nonlinear edge connecting x to z is the cause of the poor observability of the z variable of Rössler system, as discussed in previous examples. △

6 Analysis of Related Works

This section reviews the extensions and criticism in the literature regarding the aforementioned methods of *topological observability*. Most earlier discussions in the study of controllability and observability of network systems focused mainly on controllability rather than observability. However, due to the duality of these properties, there is no harm or loss of generality in comparing and discussing methods designed for controllability or observability of linear dynamical systems.

In this review, we are more interested in a broader class of works that propose metrics designed for *generalized networks*—that is, networks with no specific class of network topology or nodal dynamics (only linear and nonlinear distinctions). Nevertheless, several works in the literature explore the relation of observability and the graph properties of certain types of network topologies, including Cartesian grid graph (Notarstefano and Parlangeli 2013), chain and cycle graph (Parlangeli and Notarstefano 2012), clustered networks (Ruths and Ruths 2014), and specific complex network models, such as the scale-free network (Fu et al. 2016). The discussion of observability has also been directed to networks of specific dynamics and applications, such as Boolean networks (Chen and Qi 2009; Gates and Rocha 2015; Laschov et al. 2013), chemical reactions (Liu et al. 2013), traffic networks (Castillo et al. 2008), biological systems (e.g., neuronal networks (Gu et al. 2015; Su et al. 2017)),

and power systems (Monticelli and Wu 1985; Baldwin et al. 1993).

Lin's topological definition of controllability Lin (1974)'s definition of structural controllability (see Sect. 5.1) allows an intuitive analysis of a given *linear* dynamical system from its corresponding graph representation. This approach, which we refer to as topological controllability (observability), is not concerned with the specific entries of system matrices (A, B, C, D) such as the Kalman rank condition in Theorem 1, but rather if those matrices present a structure that *might* allow controllability under a correct and arbitrary choice of parameters. Lin argues that, in a mathematical model of a real process, the parameters estimations are contaminated by uncertainties whereas "zero" entries are practically guaranteed. Thus, a first step towards deciding if a system is controllable is to establish if it is structurally and topologically controllable.

Liu and coworker's controllability of complex networks Liu et al. (2011), motivated by the fact that complex networks often have a reliable topological (graph) representation, but an unreliable estimation of edge weights, took advantage of Lin's topological approach to investigate controllability in complex networks. Based on the maximum matching of the corresponding graph, Liu et al. (2011) identify the "minimum" set of driver nodes $\mathcal{D}$ to render a complex network structurally controllable. However, Lin's definition of structural controllability is a *crisp* definition, so how can one assure that this $\mathcal{D}$ provided by the maximum matching is really the *best* set? This is specially true since the maximum matching set of a graph is not necessarily unique. It is shown that Liu and coworkers' controllability (Liu et al. 2011) and observability (Liu et al. 2013) methods underestimate the required set of driver (Gates and Rocha 2015; Leitold et al. 2017; Wang et al. 2017) and sensor (Haber et al. 2018; Montanari and Aguirre 2019) nodes—mainly because they do not consider the specific entries of (A, B, C, D). Perhaps a more relevant question rather than if a network is structurally controllable is if it is almost uncontrollable (Friedland 1975; Cowan et al. 2012).

Control via "control hubs" A fundamental result of Liu et al. (2011) is that heterogeneous and sparse networks are harder to control than homogeneous and dense ones. This result is based on an analysis of correlation between the number of driver nodes n_{D} required for controllability and the network degree distribution, which was further discussed by Pósfai et al. (2013). This led to a counter-intuitive notion that high-degree nodes, also called *hubs*, are less desirable to be driver nodes (Liu et al. 2011). As discussed by Nepusz and Vicsek (2012); Slotine and Liu (2012), this is a consequence of the fact that, since network models in (Liu et al. 2011) do not consider nodal dynamics, the control signal injected by driver nodes spread homogeneously among its neighboring nodes, raising symmetries that restrict the state-space exploration.

Nepusz and Vicsek (2012) show that control by nodes of high degree is also possible if a different paradigm is taken: to change the analysis from nodal dynamics to *edge dynamics* (see also (Pang et al. 2017)). The argumentation follows that by choosing a hub node as a driver, if one can control its edge dynamics individually instead of its nodal dynamics, then the spread of control signals no longer suffers from symmetry issues. In case of controlling edge dynamics, homogeneous and dense networks become harder to control than heterogeneous and sparse ones. Moreover, one can benefit from controllability metrics (and other network metrics) designed for nodal analysis by performing a transformation from nodal dynamics representation to edge dynamics (that is, drawing a *line graph* from the original graph). This approach reduces the number of driver nodes in exchange for a higher control energy cost per driver node.

Influence of nodal dynamics Contradicting some claims in (Liu et al. 2011; Nepusz and Vicsek 2012), Cowan et al. (2012) affirm that the minimum number of driver nodes is not mostly dependent on node degree distributions (at least in linear networks), but rather on the underlying nodal dynamics of the studied system. Indeed, in the network modeling of Liu et al. (2011), the individual nodes of the studied benchmarks show no independent behavior, acting as pure integrators if the network were fully disconnected. This is a consequence of Liu et al. (2011) not including the presence of *self-edges*, which are a fundamental part of a network dynamics. Consider a linear dynamical network (1), rewritten as

$$\dot{x}_i = \lambda_i x_i + \sum_{j=1}^{m} a_{ij} x_j + \sum_{j=1}^{p} b_{ij} u_j, \tag{36}$$

for $i = 1, \ldots, N = m$, where x_i is the state at node v_i (only 1-dimensional systems are considered at each node). A simplified form of (3), Eq. (36) highlights that, in a dynamical network, each node has its dynamics described not only by its neighboring interactions (which includes a potential self-edge a_{ii} related to the network topology and usually translated in the Laplacian matrix, if $a_{ij} \neq 0$), but also by its own independent dynamical behavior—given by an eigenvalue λ_i that determines its individual time constant (when absent of external influences).

If all nodes of a dynamical network include self-edges, then all nodes are matched according to Definition 7. The network is referred as perfectly matched and, according to Theorem 4, the number of driver nodes required to render it structurally controllable is *one*—as long as this unique driver node is attached to *all nodes* (Cowan et al. 2012). Once more, hub nodes are shown to be fundamental for network control, despite demanding higher control energy costs. Although a

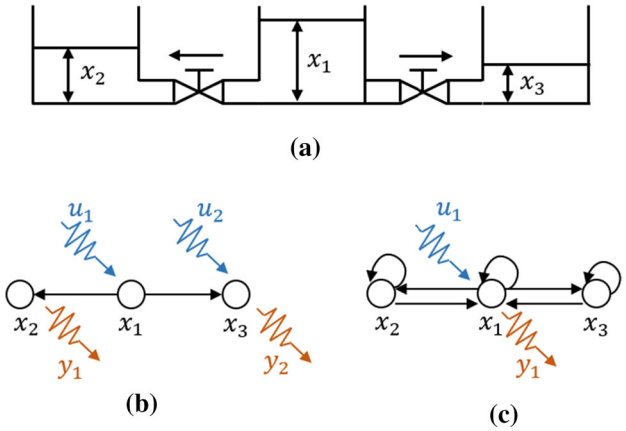

Fig. 7 Adapted from (Leitold et al. 2017). **a** Tank system. **b** Liu and coworker's representation based exclusively on the network topology, which is given by the water flow in the tank system. **c** Dynamical network representation where both the network topology and dynamics are taken into account

single control input might be sufficient to (theoretically) render a network structurally controllable, one should not expect it to be feasible from a practical point-of-view as the system dimension increases. This is related to the problem of dynamical controllability (observability).

Benchmarks studied in (Liu et al. 2011). A common topic of criticism to Liu et al. (2011)'s work is that the networks used as benchmarks for the proposed maximum matching method (see (Liu et al. 2011, Table 1)) were analyzed on an exclusively topological level while the internal states that describe the nodal dynamics were disregarded. Consider the tank system example in Fig. 7, as originally discussed in Leitold et al. (2017). Figure 7b shows a minimum set of driver nodes given by a maximum matching search if a network model is purely represented on a topological level, as Liu et al. (2011) did in most of their benchmark models. Figure 7c, on the other hand, shows this same outcome if a network model is built from the dynamical matrix that describes the underlying process, according to Cowan et al. (2012); Leitold et al. (2017); Aguirre et al. (2018). Note that, when including the network dynamics, only one driver and sensor is (theoretically) required, a result in line with the argument raised by Cowan et al. (2012).

The results pointing to a correlation between node degree distributions and (structural) controllability, therefore, can be misleading since the benchmark studied on (Liu et al. 2011, Table 1) *do not* represent dynamical processes at all. In fact, Fig. 7 is only a simple example that, if the network dynamics were considered when dealing with systems such as food webs, regulatory networks, power grids, electronic circuits, neuronal networks, and metabolic systems, it is expected that the minimum set of driver nodes would be significantly different from the results found by Liu et al. (2011). Moreover, specially for strongly connected and diffusively coupled networks, a maximum matching search can lead to a single sensor node being capable of rendering the *whole* dynamical network structurally observable, even if it has hundreds or thousands of nodes. Once again, this kind of result questions the feasibility of structural controllability and observability approaches to the control and state estimation of such types of real-world networks. A more in-depth discussion is presented in Sect. 8

Further works related to topological observability Despite the criticism regarding the limitations of using graph approaches to determine the controllability or observability of a network system, a lot of effort has been devoted to this front for three main reasons: (i) the plainness from which the graph approach proposed by Lin (1974) can be extended to the context of network systems, (ii) the high scalability of such approach to large-scale networks with thousands of nodes, as seen in Liu et al. (2011), and (iii) the fact that the recent and relevant studies established several conclusions on the effects of network structure to the controllability and observability of a system. Numerous extensions to Liu and colleagues' work led to results on target control (Gutiérrez et al. 2012; Nacher and Akutsu 2013; Jia et al. 2013; Gao et al. 2014), study of correlations between controllability and network properties (Pósfai et al. 2013; Li et al. 2017), analysis of the relationship between control energy and the chosen set of driver nodes (Yan et al. 2015), novel controllability methods based on graph properties (Leitold et al. 2017), robustness analyzes to cascading failures (Pu et al. 2012), and recent developments in network control of neuronal networks (Gu et al. 2015; Su et al. 2017).

Lack of validation A common problem in studies involving network systems and novel controllability and observability proposals is the lack of an "independent" validation. Many algorithms and techniques are applied to network databases and compared to other metrics, leading to conclusions regarding which method provides the smaller set of driver (sensor) nodes (Liu et al. 2011; Nepusz and Vicsek 2012; Liu et al. 2013; Yuan et al. 2013). However, the relevance of the provided set of driver nodes is not usually questioned. Is it the smaller set of driver nodes really *better* than the larger one? In which sense should "better" be understood? This question is a matter resolved by dynamical observability metrics, although most, if not all, are only applicable to systems of lower dimensions.

Using a first-order (linear) electronic circuit interconnected by a chain graph as a validation benchmark, Wang et al. (2017) gave attention to this topic when studying the practical feasibility of two methods to determine the minimum set of driver nodes: the maximum matching algorithm proposed by Liu et al. (2011), and the "exact" controllability method proposed by Yuan et al. (2013). The authors noticed that, when applying a single control signal to one of the chain

extremities, the longer the "control chain,"[11] the closer to being singular was the *controllability Gramian* (dual to (16)). This is an expected result since, as mentioned in Sect. 4.1, the smallest and largest eigenvalues of the controllability Gramian are related to the maximum and minimum energy costs (also known as control energy) of driving a system state through the state space. Indeed, in order to compare the practical (physical) capability of a set of driver nodes to control a dynamical system, Wang et al. (2017) investigated the conditioning number of the controllability Gramian (Definition 3) conveyed by each set of driver nodes. This is, essentially, a dynamical observability approach to this problem. One interesting result is that it is possible to raise the coefficient of controllability by a slight addition of driver nodes along the network chain, "breaking" the long control chain into smaller sections.

Indeed, when validating the feasibility of a minimum set of driver to actually control the system state, a frequent conclusion is that controllability metrics based on graph-theoretical (topological) approaches, such as (Lin 1974; Liu et al. 2011), usually underestimates the minimum set of driver nodes (Gates and Rocha 2015; Leitold et al. 2017; Wang et al. 2017). This conclusion is also present in the context of observability, where a minimum set of sensor nodes determined by the GA method (Liu et al. 2013) was shown to be insufficient to provide a reliable estimation of the system states when using Bayesian filtering techniques (Haber et al. 2018; Montanari and Aguirre 2019).

An interesting approach to validate controllability metrics is to use Boolean networks, since they highlight the interaction between the network topology and nonlinear dynamics involving simple binary variables (Gates and Rocha 2015). Moreover, Gates and Rocha (2015) show that the controllability predicted by the maximum matching method might fail even for (linearized) small nonlinear examples. Likewise, Aguirre et al. (2018) show that the structural observability defined by GA is susceptible to failures if the procedures do not take into account the nonlinearity of the edges (Aguirre et al. 2018; Letellier et al. 2018)—as discussed in Example 4.

7 Future Research Directions on the Dynamical Observability of Network Systems

Most *topological* observability methods are mainly concerned with distinguishing which set of sensor nodes renders a network system observable. Another important goal is to quantify if a given set of sensor nodes renders a network more or less observable than another set—noting that the network is observable from both sets—, and how this quantification is related to practical purposes (trajectory reconstruction, state estimation, differential embedding, and so on). This is a matter of *dynamical* observability, which still is an open problem in the literature.

A natural approach, for instance, to measure the degree of observability of a given set of sensor nodes is to extend or simply apply the dynamical observability metrics discussed in Sect. 4 to network systems. Indeed, this approach was pursued in some works in the literature. Based on the smallest eigenvalue of the Gramian (see Sect. 4.1), Yan et al. (2012) focused on the study of scaling laws for the control energy of network systems as a function of the control horizon, while Pasqualetti et al. (2013)—supported by the findings of Sun and Motter (2013)—studied the trade-offs between control energy and the number of control nodes. Gu et al. (2015) directed their study to a neuronal network application, and Bof et al. (2017) demonstrated a relation between the controllability of a network and its eigenvector centrality,[12] showing that it is harder to control a network whose nodes have a similar centrality degree. Another interesting result is the report of a trade-off between the controllability of complex networks and its resilience to perturbations and failures (Pasqualetti et al. 2018; Zhao and Pasqualetti 2019). Following Definition 4, Whalen et al. (2015) investigated the presence of symmetries in small motifs ($|\mathcal{V}| = 3$) and its restrictions on the "state-space exploration".

However, one of the reasons that led graph-inspired (topological) techniques discussed in Sect. 5 to dominate this field of work in place of matrix-theoretical ones is the high scalability of graph tools compared to those developed in control theory. Moreover, when dealing with driver (sensor) node selection, most developed solutions suffer from dimensionality issues, since they are either based on combinatorial or non-scalable optimization techniques, or heuristic approaches that are limited to the specific studied systems and show no guarantees of control (Pasqualetti et al. 2013).

In light of this open problem, in this section, we investigate some interesting paradigms to quantify observability (controllability) of network systems in a computationally feasible way. In what follows, we briefly discuss five interesting alternatives to quantify observability (controllability) in network systems.

(i) Network partitioning Formally, network partitioning consists of dividing the set of nodes $\mathcal{V}$ of a given graph $\mathcal{G} = \{\mathcal{X}, \mathcal{E}\}$ into P disjoint sets $\mathcal{P} = \{\mathcal{X}_1, \ldots, \mathcal{X}_P\}$, where $\mathcal{G}_i = \{\mathcal{X}_i, \mathcal{E}_i\}$ is the ith subgraph of $\mathcal{G}$, for $i = 1, \ldots, P$.

[11] The "control chain" here refers to the path of nodes between the driver node (the input signal) and the target node.

[12] It must be noted, however, that this relation was established based on an assumption that the dynamic matrix A is non-negative, which is not generally the case when the nodal dynamics are taken into account. When studying combustion and biological networks, Haber et al. (2018) detected no clear correlation between the optimal selection of sensor nodes and the corresponding node centrality measures.

Clearly, network partitioning methods (Fortunato 2010) are a viable alternative in network systems to subdivide a high-order systems into several and, if possible, non-intersected "clusters" of lower dimension. Ideally, the low-order subgraphs could be assessed by traditional methods from control theory. In practice, however, to subdivide a network into independent systems, or even to uncover its remaining dynamical interdependences, might be a challenge. For instance, Liu et al. (2013) proposed a sensor selection method based on a network partitioning into SCC (Sect. 5.2). Desynchronized (partitioned) control has also been implemented by Su et al. (2017) to validate its experiments.

For instance, following the GA method, Pasqualetti et al. (2013) proposed an elegant solution to actuator placement by choosing all nodes at each SCC boundaries[13] as driver nodes. Hence, the authors developed a control law strategy that *decouples* the SCC dynamical interdependences in such a manner that its selected "internal" driver nodes are solely responsible for the SCC steering from the origin to a target state. In fact, by "forcing" all the SCC to behave independently, the high-order network problem is reduced to independent low-order dynamical systems that can be controlled by local control centers. The authors argue that their method is scalable since it depends on the number of partitions rather than the network cardinality. By breaking the network in partitions with a sufficiently small cardinality, actuators (sensors) can be optimally placed in each partition such that a given dynamical controllability (observability) measure is maximized by brute-force search.

Although the aforementioned method, as well as other network partitioning methods, are tempting, highly centralized networks are not suitable for decomposition. In such cases, even if SCC can still be identified, their subgraphs might still be very high-order systems for traditional techniques of control theory.

(ii) Set function optimization Summers et al. (2016) formulated the sensor[14] placement problems as a *set function* optimization problem as follows:

$$\max_{\mathcal{S}\subseteq\mathcal{X},|\mathcal{S}|=q} J(\mathcal{S}), \tag{37}$$

where given a $\mathcal{X} = \{x_1, \ldots, x_n\}$, the problem is to select a q-element subset $\mathcal{S}$ of $\mathcal{X}$ that maximizes an objective set function $J(\mathcal{S}) : 2^n \rightarrow \mathbb{R}^1$—i.e., a function that assigns a real number to each subset $\mathcal{S}$. The objective function desired to be maximized is chosen so that it describes the trade-off between the number of required sensor nodes and the related estimation energy costs. Possible functions are the dynamical observability metrics discussed in Sect. 4.1. As one might note, (37) is a combinatorial optimization problem that could only be solved by brute force search if the network dimension were of lower order.

The greatest contribution of Summers et al. (2016) is to show that most dynamical observability metrics based on the observability Gramian are *submodular* functions. Thus, although solving the optimization problem through brute-force search is computationally hard, if the objective function is submodular, then the optimization problem can be solved by a greedy algorithm with guaranteed performance (Nemhauser et al. 1978). Via numerical simulations, the authors show that, considering $|\mathcal{V}| = 25$ and $|\mathcal{S}| = 7$, the greedy optimization displays a result better than 99.93% of all other combinations. The method is further validated on a power system model and scalability of the greedy algorithm is discussed in detail. Haber et al. (2018) apply, for comparison purposes, Summers and coworkers' approach to nonlinear networks and show that their method performs well, although they do not provide any mathematical proofs for the nonlinear case.

(iii) Symbolic observability To deal with larger systems with more complicated dynamics, Letellier and Aguirre (2009); Bianco-Martinez et al. (2015) provided a dynamical symbolic observability metric that does not depend on the specific parameter entries but rather on the presence and quantity of linear, nonlinear and rational couplings within the dynamical system. The observability metric is normalized in a [0, 1] range, allowing one to compare different dynamical systems—which is not possible following Definition 4. This approach seems to be promising for dynamical networks as long as they are"not very large" (Letellier et al. 2018).

Some other interesting symbolic approaches to quantify observability have been presented in a power system analysis context (Slutsker and Scudder 1987; Bretas and London 1998). Indeed, the problem of sensor and actuator placement in power systems is a very relevant (and old) one due to emerging and expensive technologies designed to monitor or control the system states (Monticelli and Wu 1985; Baldwin et al. 1993). An application example to power systems is given in Sect. 8.

(iv) Indirect measures of "reconstruction quality" In an observability context, the degree of observability can be indirectly assessed through the "estimation quality" of the state. This is a more empirical approach. For instance, in a Bayesian filtering context, this is motivated by the fact that if the measured signals do not provide relevant information to the filter, i.e., they convey poor observability, then the update stage of the filter is impaired and, consequently, the estimates show poor performance. This is based on an assumption that the filters or algorithms are well-tuned (Montanari and Aguirre 2019).

[13] See (Pasqualetti et al. 2013) for a mathematical definition.

[14] It was actually formulated in the context of controllability and optimal actuator placement.

Examples found in the literature are the estimation error of a moving horizon estimation technique (Haber et al. 2018) or a particle filtering framework (Montanari and Aguirre 2019), as well as the fitting error from training a Gauss-Newton algorithm (Guan et al. 2018) or a reservoir computer (Carroll 2018). Due to the scalability issues of Bayesian filtering methods and similar techniques, this approach is not very useful for networks with dimensionality $N \gg 100$. It is an interesting approach to further understand the interplay between observability, network topology, and nodal dynamics (Guan et al. 2018; Montanari and Aguirre 2019).

Note that, all discussed observability metrics throughout the text depend on knowledge of the system equations. When such are not available, Aguirre and Letellier (2011) provided a data-based procedure to infer the degree of observability from a recorded time series. This approach relies on measuring the reconstruction quality from a embedding of the available time series as a function of specific properties associated with poor coefficients of observability, such as sharp folds and strong squeezing of trajectories as consequence of singularity issues.

(v) Observability of a subset of nodes of interest As discussed, a recurring goal in the literature is the search of an optimal set of sensor nodes that renders a dynamical network fully observable. Motter (2015) argues that this goal is not quite realistic, though, since, from a practical point-of-view, to reconstruct the dynamical system trajectory of a high-dimensional system requires direct measurement of most nodes in a network—which is not always feasible. An alternative, therefore, is to focus on a particular subset of nodes of interest and determine what is the required set of sensor nodes in order to render this subset observable. Basically, this approach revolves around reducing the dimensionality of the problem. This problem has been explored by Iudice et al. (2019) in the context of node observability (controllability), i.e., focusing on a particular node observability. We are particularly working on expanding this approach to determine the observability of a subset of nodes, based on a concept known as functional observability, from control theory (Jennings et al. 2011; Hieu and Tyrone 2012). Analogously, Gao et al. (2014) explored the concept of "target controllability," based on the definition of output controllability from control theory, where one is interested in steering only a specific subset of nodes of interest in the network. Note that the concepts of functional observability and output (target) controllability, albeit related, are not dual.

8 Application Examples

Throughout the text, we showed how the concepts of structural, dynamical, and topological observability can be applied to a (low-dimensional) nonlinear dynamical system, the Rössler system. In the following, we provide an example of how these concepts are applied in the high-dimensional context of power grids and multi-agent coordination. Moreover, we also take this opportunity to show how the studied dynamical systems can be modeled in a network context.

It should be mentioned, however, that since the numerical computation of the observability matrix (22) of a nonlinear model is quite unfeasible in a high-dimensional setting, we focus on a linearized model of the nonlinear network dynamics around the operation point. In what follows, to determine the "minimum set of sensor nodes $\mathcal{S}$" using the maximum matching search (Sect. 5.1.1), we use its MATLAB-based implementation found in the NOCAD toolbox (Leitold et al. 2019).

8.1 Power Grids

Model dynamics This section provides an application example in a IEEE power grid benchmark with 50 generators and 145 buses (Vittal 1992; Nishikawa and Motter 2015). Figure 8a illustrates the benchmark model as network system. In this context, the power grid dynamics are modeled as a network of interconnected Kuramoto oscillators (Arenas et al. 2008; Dorfler et al. 2013), given by

$$\frac{2H_i}{\omega_R}\ddot{\phi}_i + \frac{D_i}{\omega_R}\dot{\phi}_i = P_i + \sum_{j=1, j\neq i}^{m} K_{ij} \sin\left(\phi_j - \phi_i + \beta_{ij}\right), \tag{38}$$

for $i = 1, \ldots, m$, where m is the number of nodes, $\phi_i(t)$ is the phase angle of oscillator v_i at time t relative to a frame that rotates at the reference frequency ω_R rad/s, H_i and D_i are inertia and damping constants, respectively, P_i is related to the power supply of generator at node v_i, K_{ij} is the coupling weight related to the maximum power transfer capacity in the respective transmission line interconnection two nodes (v_i, v_j), and β_{ij} is the corresponding phase shift.

All parameters are estimated from the power grid benchmark dataset provided by Vittal (1992) following the "effective network model" paradigm[15] described by Nishikawa and Motter (2015). While (H_i, D_i) are estimated from the generator constructive parameters, $(P_i, K_{ij}, \beta_{ij})$ are inferred from the power grid steady-state distribution of power flow. Although the power grid benchmark has 145 buses, the power grid model in (38) is reduced, via Kron reduction (Sauer et al. 2017), to an effective network[16] with $m = 50$ nodes, where

[15] Different models of power grids based on networks of coupled oscillators are discussed in (Nishikawa and Motter 2015; Moreira and Aguirre 2019).

[16] Differently from the power grid structure shown in Fig. 8, due to the Kron reduction, the effective network model is fully connected (i.e., each generator is directly connected to every other generator in the

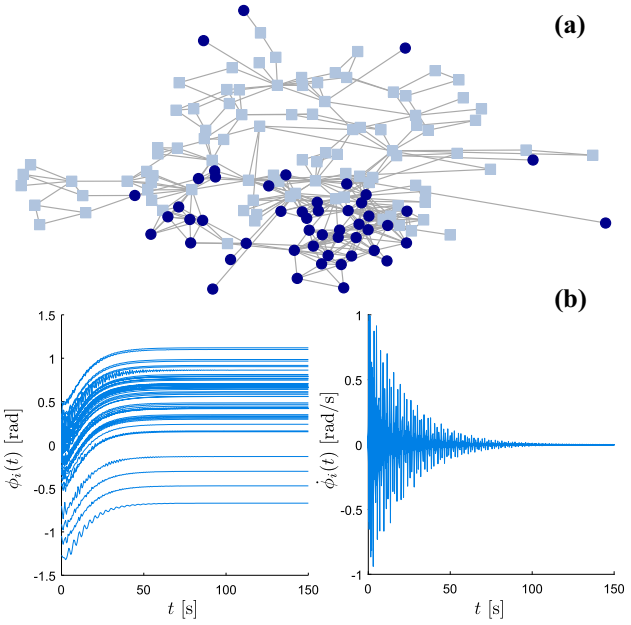

Fig. 8 **a** IEEE power grid benchmark, where generator and load buses are represented by circle and square nodes, respectively, and transmission lines by edges. **b** Phase and instantaneous frequency time evolution. Linearization is performed around the equilibrium point at $t = 150\,\mathrm{s}$

each node v_i represents a generator whose dynamics are described by a second-order Kuramoto oscillator. The power grid dynamics are shown in Fig. 8b. If $\dot{\phi}_i(t)$ converges to zero for all generators, then the power grid is said to be fully synchronized. A MATLAB implementation of this framework is provided by Nishikawa and Motter (2015).

For the following computations, model (38) is linearized around its equilibrium point (computed through numerical integration after $t = 150$ s, as in Fig. 8b). The linearized model is represented in its canonical form:

$$\begin{bmatrix} \dot{\phi} \\ \ddot{\phi} \end{bmatrix} = \begin{bmatrix} 0 & I_m \\ A_{21} & A_{22} \end{bmatrix} \begin{bmatrix} \phi \\ \dot{\phi} \end{bmatrix}, \tag{39}$$

where $\phi = [\phi_1 \ \ldots \ \phi_m] \in \mathbb{R}^m, 0 \in \{0\}^{m\times m}, A_{21} \in \mathbb{R}^{m\times m}$ is a fully dense matrix, and $A_{22} \in \mathbb{R}^{m\times m}$ is a diagonal matrix.

PMU placement One specific problem related to observability in the context of power grids is that of optimal placement of phasor-measurement units (PMU) (Phadke and Thorp 2008; Yang et al. 2012). A PMU placed on a generator bus (node) allows real-time measurement of its voltage and line currents. Moreover, depending on the power grid structure, voltages and/or line currents of neighboring buses (nodes) can be determined from Kirchhoff's law. Indeed, in the scientific community of power systems (Peng et al. 2006; Cruz and Rocha 2017; Tran and Zhang 2018), the search for an optimal PMU placement such that the voltages of all buses can be determined is known as a "topological observability" problem.[17]

Two main reasons motivate this problem. On the one hand, a PMU is a very expensive equipment, and it might not be economically viable to install one in every node of a power grid (Rocha et al. 2018). On the other hand, communication between two (geographically apart) areas might have been interrupted by some failure or malicious attack and one might need to estimate, from its accessible set of measurements, what is the state of some other generator connected to the power grid. Indeed, a reliable communication structure (which includes both direct and estimated measurements) is a very important concern for the implementation of Wide Area Control techniques, especially with the current transition of power grids to smart grids (Malik 2013).

In the following, assume that if a PMU is placed in a generator node (bus) v_i, then one has access sufficient information to infer the respective generator states $\{\phi_i, \dot{\phi}_i\}$. In this sense, the optimal PMU placement can be framed as a (traditional) observability problem in the sense that one wants to estimate, from knowledge of the generator states where a given set of PMU is placed, the generator states of all other nodes that do not have a PMU. We use this example to counterpoise the different types of observability discussed in this manuscript, stating pros and cons in each case.

Structural and topological observability Consider the linearized model (39) and that, if a PMU is placed on generator v_i, then node v_i is said to be a sensor node of $\mathcal{S}$ and hence $\{\phi_i, \dot{\phi}_i\} \in \mathcal{S}$. Since A_{21} is a fully dense matrix whose individual entries a_{ij} are related to the power system parameters $(K_{ij}, \beta_{ij}, H_i)$, the probability that the columns of $\mathcal{O}$ are linearly dependent is practically zero (as pointed out by Remark 7). This is specially true if we consider that the generator parameters and power supply levels are not homogeneous along the power grid (which is true in reality). Thus, the dynamical network (39) is topologically observable (in Lin's sense) from *any* generator node (implying that $|\mathcal{S}| = 1$ is a sufficient and necessary condition). Likewise, it is structurally observable (in Kalman's sense) from any node.

This illustrates the discussion in Sect. 6 that when nodal dynamics are taken into account, self-edges are included in the graph representation, leading to a trivial solution where

Footnote 16 continued
network, with a coupling strength K_{ij} related to their corresponding power flow).

[17] Although this problem shares the same nomenclature discussed throughout this paper, it has a different meanings. "Topological observability of power systems" is a solvability problem where one wants to determine, based on Kirchhoff's law, the whole vector of voltages and line currents from knowledge of the admittance matrix and some measurements available by a given set of PMUs. "Topological observability of dynamical systems," on the other hand, is graph-theoretical way to certify if the basic conditions for the design of a stable linear observer can be satisfied.

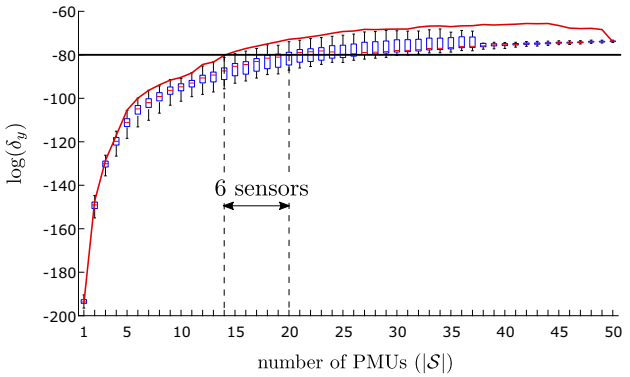

Fig. 9 Coefficient of observability δ_y per number of PMUs (sensor set cardinality $|\mathcal{S}|$), considering an optimal sensor placement (solid red line) and 1,000 Monte Carlo runs with random placements (boxplot) (Color figure online)

all nodes are matched, and thus only one sensor node (placed anywhere) is required to render the network observable. In this case, self-edges are only represented in states $\ddot{\phi}_i$ (due to the diagonal block A_{22}). Nevertheless, since there is a bidirectional connection between state variables $\dot{\phi}_i$ and $\ddot{\phi}_i$, for all i, then the conclusion remains: every node is matched. This is inline with the examples in Fig. 5.

Dynamical observability Although, in the linear case, any node is sufficient as a sensor node to render the power grid topologically or structurally observable, one might argue that, for practical purposes, $\mathcal{S}$ is almost unobservable. Indeed, if $|\mathcal{S}| = 1$, then $\delta_y \approx 10^{-85}$ (regardless of where the PMU is placed). Hence, topological and structural observability approaches do not provide any relevant insight into the problem of optimal sensor placement *in this case*.

Assessing the dynamical observability of a power system, on the other hand, might not only be useful to determine the minimum number of sensor nodes required to render the network observable from a practical point-of-view, but also to assess the optimal placement. Figure 9 shows how the coefficient of observability δ_y increases with the number of PMUs considering an optimal[18] and multiple random placements. The optimal PMU placement is based on the set function optimization problem (37). We provide a MATLAB implementation of a greedy algorithm to solve (37) at https://doi.org/10.13140/RG.2.2.22524.28803/1, as proposed by Summers et al. (2016).

It is interesting to see that the network dynamical observability δ_y greatly benefits from the first few sensor nodes (approximately 20% of the network cardinality), before reaching a stationary value (around half the network cardinality) where further sensor nodes do not increase δ_y. An interesting interpretation, discussed by Guan et al. (2018), is that as the number of sensor nodes increases, useful and relevant data about the system dynamics is acquired by the output measurements until a turning point where additional sensors provide redundant information about the system dynamics. This sudden increase in the network observability with the first few choices of sensor nodes is in line with results in (Qi et al. 2015; Summers et al. 2016; Guan et al. 2018).

Not only the network dynamical observability improves with the addition of sensor nodes, but it can also benefit from an optimal placement. Figure 9 shows the efficacy of the framework put forward by Summers et al. (2016), where the greedy algorithm approach to sensor placement provides an optimal performance clearly above random placements of the same sensors. For instance, to reach a given degree of observability (e.g., $\log(\delta_y) \approx -80$), 14 PMUs are needed if they are *optimally* placed over the power grid. On the other hand, a *random* placement requires 20 PMUs to reach (with a $\sim 50\%$ chance) the desired degree of observability.

This is especially important since a sensor placement that conveys a higher coefficient of observability δ_y is shown to be related to a better state estimation (Montanari and Aguirre 2019; Singh and Hahn 2005). Indeed, analogous to the results exposed in Fig. 9 and also in the context of PMU placement and power grids, Qi et al. (2015) showed that a PMU placement that conveys higher coefficient of observability (albeit based on the determinant of an empirical observability Gramian) to the power grid leads to a smaller state estimation error (based on a unscented Kalman filter framework).

8.2 Multi-agent Consensus

Model dynamics This section provides an application example in the context of collective behavior of locally interacting adaptive and identical individuals, hereby called agents. Examples of these agents and collective dynamics include fish in schools, birds in flocks and robots in artificial swarms. The following multi-agent system describes the general flocking behavior of a group of moving agents in a 2-dimensional space (Vicsek et al. 1995; Arenas et al. 2008; Bouffanais 2016):

$$\dot{x}_i = \frac{1}{k_{i,\text{in}}} \sum_{j=1}^{m} W_{ij}(x_j - x_i), \tag{40}$$

for $i = 1, \ldots, m$, where $x_i(t)$ is the velocity direction (angle) of agent i at time t, $k_{i,\text{in}} = \sum_j W_{ij}$ is the node in-degree of agent i, m is the number of agents, and $W \in \{0, 1\}^{m \times m}$ is an adjacency matrix that describes the signaling network between agents, where $W_{ij} = 1$ if agent i perceives or senses agent j in its neighborhood, and $W_{ij} = 0$ otherwise.

This local consensus protocol represents the decentralized information flow throughout the swarm as a behavioral

[18] Note that, it is not feasible to find the optimal placement via brute-force with a system of dimensionality $N \gtrsim 100$.

response to changes in the leading agents states.[19] The Laplacian matrix L associated with the adjacency matrix W plays an important role in this analysis since (40) can be represented as

$$\dot{\boldsymbol{x}} = -D_{\text{diag}}^{-1} L\boldsymbol{x}, \tag{41}$$

where D is the degree matrix defined in "Appendix A".

Albeit simple model (40) allows us to illustrate our discussion without straying too far from the main focus of this work. It is expected that a more specific application would also have to take into account a more detailed model.

Sensor networks Compared to the application example in Sect. 8.1, the collective motion of agents adds an extra layer to our analysis: the signaling network W between agents is not fixed, but rather time dependent. The communication between agents depends on physiological (technological) limitations of living (artificial) agents, which often constrain the sensory range that a single agent can both perceive and process in its neighborhood (Pearce et al. 2014; Bouffanais 2016). For example, the presence of obstacles forces the swarm of agents to engage in different maneuvers that essentially change the neighborhood of interactions of each single agent (Olfati-Saber 2006), re-configuring the signaling network. This is a feature that is particularly connected to the design problem of wireless sensor networks (Derakhshan and Yousefi 2019).

The optimal sensor placement in multi-agent systems, therefore, has a different motivation than in Sect. 8.1. In the present case, each agent usually has its own sensory system that assess neighboring information for decision making in a decentralized manner. From the point-of-view of a single agent, access to the whole state of a system is not needed and, therefore, there is no observability problem. On the other hand, access to the whole system state might be required for monitoring and control purposes in applications that rely on a command center, such as for unmanned aerial vehicle coordination (Olfati-Saber 2006) or cyber-attack detection in self-driving vehicles coordination (Vivek et al. 2019). Although the system state can be monitored, in principle, by transmitting the measured states of all agents to the command center, this is not energetically efficient. Battery life is one of the major limitations in artificial swarms applications, and relying on each single agent to transmit its current state to a command center has a high overall energy consumption. A more efficient alternative is to find the minimum set of agents (sensor nodes) that need to transmit their current state to a command center such that the state of the remaining agents can be estimated/reconstructed. This is an observability problem.

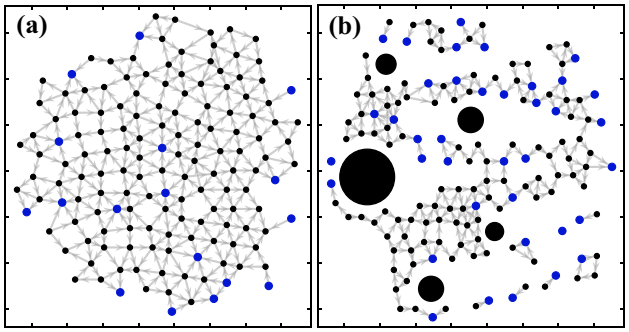

Fig. 10 Signaling network W of a flock of $m = 150$ agents moving in a 2-dimensional space in two different scenarios: **a** the agents are moving in consensus, and **b** a snapshot of the agents engaged in a split maneuver to dodge obstacles (large circles) along the way. Agents are represented by black nodes (in xy coordinates), and the minimum set of sensor nodes to render the system structurally observable (according to the maximum matching algorithm) is represented by blue nodes. The signaling networks were adapted from (Olfati-Saber 2006) (Color figure online)

Sensor Placement In multi-agent systems, the swarm of agents is continuously self-organizing in motion, changing the signaling network W as a function of the agents position over time (similar to a switching network). For instance, after a split maneuver, the system might become unobservable from a set of sensor nodes chosen before the start of the maneuver, requiring a new set of sensor nodes to be assigned for the new configuration.

Figure 10 illustrates the chosen minimum set of sensor nodes required to convey observability to the system in two different scenarios: the first when the group of agents moves in consensus as a flock, and the second when the group of agents splits apart to engage in a evasive maneuver against obstacles in its path. In this example, the minimum set of sensor nodes is determined by using the maximum matching algorithm (Sect. 5.1.1) on the graph $\mathcal{G}(A)$ associated with the dynamical matrix $A = -D_{\text{diag}}^{-1} L$ given by model (41).

Since the signaling network re-configures in real time, it is important that the minimum sensor placement algorithm is sufficiently fast for such application. For $m = 150$ agents, the maximum matching algorithm solves the minimum sensor placement problem in less than a second. Indeed, considering the present state-of-the-art, a topological observability approach is the only feasible alternative[20] to solve the minimum set of sensor nodes in real-time applications involving swarms with up to thousands of agents. This is further supported by the low complexity order $O(\sqrt{m}|\mathcal{E}|)$ predicted in a worst-case scenario.

[19] Leading agents can represent agents with privileged information about external factors, such as predators and obstacles, or agents that receive external input from a control center in artificial swarms.

[20] For example, solving the minimum sensor placement problem based on the rank condition (14) for observability was shown to be a NP-hard problem (Olshevsky 2014).

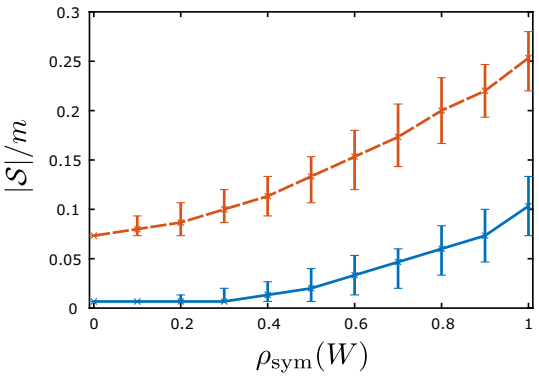

Fig. 11 Proportion of the minimum number of sensor nodes $|\mathcal{S}|/m$ as a function of the signaling network symmetry $\rho_{\mathrm{sym}}(W)$ for the two different scenarios: consensus (solid line) and split maneuver (dashed line). Simulations are presented for 1,000 Monte Carlo runs. Lines show the median values, while error bars show the 5th and 95th percentile

Observability and Network Topology We now investigate the relation between the minimum set of sensor nodes and the network topology $\mathcal{G}(A)$. It is clear that, after the split maneuver, the loss of connectivity in W increases the size of the minimum set of sensor nodes, specially because additional sensor nodes must be included to track (observe) the state of isolated agents and disconnected subgraphs. On the other hand, Fig. 11 shows that the minimum number of sensor nodes is related not only to the number of subgraphs in $\mathcal{G}(A)$, but also to the degree of symmetry $\rho_{\mathrm{sym}}(W)$ of the binary matrix W, defined as:[21]

$$\rho_{\mathrm{sym}}(W) = \frac{\text{number of unidirectional edges in } \mathcal{G}(W)}{\text{number of edges in } \mathcal{G}(W)}. \quad (42)$$

The lower the symmetry of the signaling network, the larger the minimum sensor set. This is a straight consequence of the changes in the graph topology: a lesser symmetry reduces the number of paths between nodes, and also increases the number of dilations in the graph, therefore requiring a higher number of sensor nodes to guarantee structural observability in Lin's sense (Theorem 3). Likewise, reducing the adjacency matrix symmetry (changing bidirectional edges to unidirectional edges) also increases the number of unmatched nodes (as seen in Fig. 5c,d), increasing the number of sensor nodes determined by the maximum matching algorithm.

If W is symmetric (and $\mathcal{G}(W)$ is undirected), as discussed in Sect. 8.1, any agent can be chosen as a sensor node, regardless of the network size and topology. This raises once again the question of whether a structural or topological approach to observability is sufficient to determine the minimum set of sensor nodes for practical purposes. Nevertheless, Fig. 11 suggests that, as W becomes more asymmetric, determining the minimum set of sensor nodes becomes a more complicated problem which a topological approach helps to shed some light on it. For instance, Fig. 11a shows that the studied multi-agent system in consensus can be rendered observable by assigning less than 10% of the total number of agents as sensors regardless of the level of symmetry. Although the study of controllability of multi-agent systems has found several advances in recent years (Rahmani et al. 2009; Komareji and Bouffanais 2014; Guan and Wang 2018), we emphasize that studying the topological observability of multi-agent systems, such as the work of Lu et al. (2017), can lead to novel developments in different fields, including swarm monitoring applications, development of cyber-defense protocols, and optimal configuration of sensor networks.

[21] A symmetric adjacency matrix corresponds to an undirected graph, which only has bidirectional edges. Contrariwise, an asymmetric adjacency matrix is related to a directed graph, which has unidirectional (and possibly bidirectional) edges.

9 Conclusion

In this manuscript, we reviewed some definitions of *observability* of dynamical systems, as far as network systems are concerned. Firstly, we presented the traditional concepts of observability proposed by Kalman (and its following extension to nonlinear systems), where a system is classified simply as observable or unobservable. We classify this approach as *structural observability*. However, due to numerical issues, a set of outputs that renders a system observable, but badly conditioned, might not provide a satisfactory state reconstruction under a practical context. Thus, a more relevant question arises: whether an observable system is *almost unobservable*. Several indices were proposed in the literature to quantify the quality of observability of a linear and nonlinear system. We refer to this continuous quantification of observability as *dynamical observability*.

In a network context, traditional control methods usually fail to be applied due to high-dimensionality issues, especially when nonlinear systems are considered. This is also true in an observability context, leading to the need for novel methods that circumvent this problem. The intuitive modeling of network systems via graph representations led to a new set of observability methods that benefits from the network topology properties to derive the minimum set of sensor nodes under which a network is rendered observable. We classify this approach as *topological observability*.

Although intuitive and suitable for high-dimensional network systems, these topological observability metrics have several limitations under a practical context, especially when the nodal dynamics are considered. Indeed, we provide a critical review of the recent progress in the study of observability (and controllability) of network systems, emphasizing the main advantages (e.g., its high scalability and interpretability) and disadvantages (e.g., the underestimation of

the necessary set of sensor nodes under a practical context) of topological observability. To circumvent the main disadvantages in the study of observability of network systems, we briefly review some interesting apporaches in the literature in order to provide future research directions of interest in this field.

Finally, we show and discuss in two application examples how the concepts of structural, dynamical, and topological observability can aid in the problem of sensor placement. In power grids, since all nodes are diffusively coupled according to a full network and self-edges are represented, topological observability (and structural) is easily achieved with any single choice of sensor node. Thus, a dynamical observability is necessary not only to distinguish which choice of sensor node is the best, but also to determine what is the smallest number of sensor nodes so that the degree of observability of the power system reaches a satisfactory value (where it stops growing). On the other hand, a topological approach provides the only highly scalable solution to cope, nowadays, with real-time applications in multi-agent consensus.

As a general conclusion, we argue that, contrariwise to some recent results in the literature, depending on the characteristics of the network system, a topological or structural approach to observability might not "tell the full story," requiring a further investigation based on dynamical observability. It is suggested that the less directed a network is and the higher the number of self-edges in its topology, the more a topological observability underestimates the set of sensor nodes.

Acknowledgements The authors would like to thank Petrus E. Abreu and Ercilio I. Moreira for the insightful discussions. ANM acknowledges financial support from Coordenação de Aperfeiçoamento de Pessoal de Nível Superior (finance code 001). LAA acknowledges Conselho Nacional de Desenvolvimento Científico e Tecnológico (Grant No. 302079/2011-4).

Compliance with Ethical Standards

Conflict of interest The authors declare that they have no conflict of interest.

A Graph Structures and Properties

The following conventions and properties of graph theory are used throughout this work. For more details, we refer the reader to (Newman 2010; Chen et al. 2013; Bullo 2016). Figure 12 illustrates the following types of graph and exemplifies some usual graph structures in the literature:

- *Undirected and directed graphs.* If (v_i, v_j) are undirectedly linked, then $a_{ij} = a_{ji} \neq 0$, and A_{adj} is a symmetric matrix. If (v_i, v_j) are not linked, then $a_{ij} = 0$. This adjacency matrix is denoted as *undirected*. If it is a *directed* graph, or *digraph* for short, then a_{ij} corresponds to an edge connecting node v_j to node v_i (Newman 2010). If $a_{ii} \neq 0$, then node i has an edge connecting to itself, denoted as *self-edge*.
- *Binary and weighted graphs.* If $A_{\text{adj}} \in \{0, 1\}^{m\times m}$, then the graph is *binary* or *unweighted*. And the graph is *weighted* if $A_{\text{adj}} \in (-\infty, \infty)^{m\times m}$.
- *Paths.* A *path* is an ordered sequence of nodes, interconnected by direct edges (if it is a digraph), between a given pair of nodes. A *simple path* has no repeated node in its sequence, except possibly for the initial and final node.
- *Cycle.* A *cycle* is a simple path where the final node equals the inital one, and it has at least 3 nodes. Otherwise, the graph is *acyclic*.
- *Connected.* A graph is *connected* if there exists a path between any pair of nodes.
- *Subgraph.* A digraph $\mathcal{G}' = \{\mathcal{V}', \mathcal{E}'\}$ is a subgraph of $\mathcal{G}$ if $\mathcal{V}' \subseteq \mathcal{V}$ and $\mathcal{E}' \subseteq \mathcal{E}$.

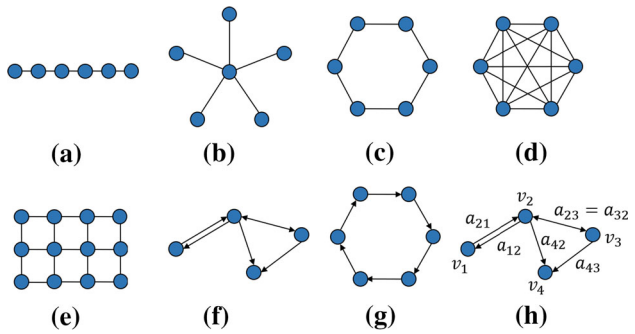

Fig. 12 Graph examples. **a** Chain or path graph. **b** Star graph. **c** Ring or cycle graph. **d** Complete or fully connected graph. **e** Cartesian grid graph. **f** Digraph. **g** Cycle digraph. **h** Weighted graph

In a dynamical system context, the Laplacian matrix and the connectivity properties of a graph are very useful in the state-space representation of networks of diffusively coupled oscillators (Bullo 2016). These concepts are reviewed in what follows:

- $\mathcal{G}$ is *strongly connected* if there exists a directed path between any pair of nodes;
- $\mathcal{G}$ is *weakly connected* if the undirected version of a digraph is connected;
- A *globally reachable node* is a node that can be reached from any node by a direct path; and
- A *directed spanning tree* is a subgraph where a node is the root of directed paths to all other nodes.

A particular definition of interest is the *strongly connected components* (SCC). A subgraph $\mathcal{G}'$ is a SCC if $\mathcal{G}'$ is strongly

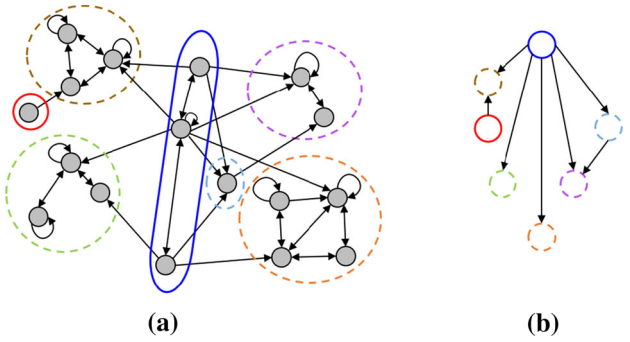

Fig. 13 **a** SCC (in dashed circles) and root SCC (in solid circle) of a digraph. **b** Condensation graph of (**a**). Adapted from (Bullo 2016)

connected and any subgraph of $\mathcal{G}$ strictly containing $\mathcal{G}'$ is not strongly connected. A *root SCC* is a SCC with no incoming edges. A *condensation digraph* $C(\mathcal{G})$, in turn, is defined as a graph whose nodes are a SCC of $\mathcal{G}$, and there exists a directed edge from a node formed by $\mathcal{G}'_1$ to a node formed by $\mathcal{G}'_2$ if there exists a node from $\mathcal{G}'_1$ connected to a node from $\mathcal{G}'_2$. Figure 13 illustrates these concepts.

The Laplacian matrix $L = [l_{ij}]$ is defined as follows:

$$L = D_{\text{diag}} - A_{\text{adj}}, \tag{43}$$

where $D_{\text{diag}} = \text{diag}(k_{1,\text{in}}, \ldots, k_{m,\text{in}})$ is called the degree matrix and $k_{i,\text{in}} = \sum_{j=1}^{m} a_{ij}$ is the in-degree of node v_i. Some useful properties of the Laplacian matrix are Boccaletti et al. (2006):

- L is always symmetric and positive semidefinite.
- Given that $\lambda_1 \leq \lambda_2 \leq \ldots \leq \lambda_m$ are eigenvalues of L, if $\lambda_2 > 0$ ($\lambda_1 = 0$), then the network is connected.

Based on the type of graph under study, several interesting conclusions can be derived from the structure or connectivity properties of a graph, which can be measured by graph and complex network metrics. The reader is referred to Costa et al. (2007), Chen et al. (2013)) for further details on network metrics.

References

Aguirre, L. A. (1995). Controllability and observability of linear systems: Some noninvariant aspects. *IEEE Transactions on Education*, *38*(1), 33–39.

Aguirre, L. A., & Letellier, C. (2005). Observability of multivariate differential embeddings. *Journal of Physics A: Mathematical and General*, *38*(28), 6311–6326.

Aguirre, L. A., & Letellier, C. (2011). Investigating observability properties from data in nonlinear dynamics. *Physical Review E*, *83*, 066209.

Aguirre, L. A., Bastos, S. B., Alves, M. A., & Letellier, C. (2008). Observability of nonlinear dynamics: Normalized results and a time-series approach. *Chaos*, *18*, 013123.

Aguirre, L. A., Portes, L. L., & Letellier, C. (2018). Structural, dynamical and symbolic observability: From dynamical systems to networks. *PloS ONE*, *13*(10), e0206180.

Arenas, A., Díaz-Guilera, A., Kurths, J., Moreno, Y., & Zhou, C. (2008). Synchronization in complex networks. *Physics Reports*, *469*(3), 93–153.

Baldwin, T., Mili, L., Boisen, M., & Adapa, R. (1993). Power-system observability with minimal phasor measurement placement. *IEEE Transactions on Power Systems*, *8*(2), 707–715.

Barabási, A. L. (1999). Emergence of scaling in random networks. *Science*, *286*(5439), 509–512.

Barabási, A. L. (2009). Scale-free networks: A decade and beyond. *Science*, *325*(5939), 412–413.

Barabási, A. L., & Pósfasi, M. (2016). *Network science* (1st ed.). Cambridge: Cambridge University Press.

Bianco-Martinez, E., Baptista, M. S., & Letellier, C. (2015). Symbolic computations of nonlinear observability. *Physical Review E*, *91*, 06912.

Boccaletti, S., Kurths, J., Osipov, G., Valladares, D., & Zhou, C. (2002). The synchronization of chaotic systems. *Physics Reports*, *366*(1–2), 1–101.

Boccaletti, S., Latora, V., Moreno, Y., Chavez, M., & Hwang, D. U. (2006). Complex networks: Structure and dynamics. *Physics Reports*, *424*(4–5), 175–308.

Bof, N., Baggio, G., & Zampieri, S. (2017). On the role of network centrality in the controllability of complex networks. *IEEE Transactions on Control of Network Systems*, *4*(3), 643–653.

Bouffanais, R. (2016). *Design and control of swarm dynamics*. Berlin: Springer.

Bretas, N., & London, J. (1998). Network observability: The critical measurement identification using the symbolic Jacobian matrix. In *POWERCON'98 1998 international conference on power system technology proceedings* (pp. 1222–1226)

Bullo, F. (2016). Lectures on network systems. CreateSpace

Carroll, T. L. (2018). Testing dynamical system variables for reconstruction. *Chaos*, *28*, 103117.

Castillo, E., Jiménez, P., Menéndez, J. M., & Conejo, A. J. (2008). The observability problem in traffic models: Algebraic and topological methods. *IEEE Transactions on Intelligent Transportation Systems*, *9*(2), 275–287.

Chapman, A., Nabi-Abdolyousefi, M., & Mesbahi, M. (2014). Controllability and observability of network-of-networks via cartesian products. *IEEE Transactions on Automatic Control*, *59*(10), 2668–2679.

Chen, C. T. (1999). *Linear system theory and design* (3rd ed.). Oxford: Oxford University Press.

Chen, D., & Qi, H. (2009). Controllability and observability of Boolean control networks. *Automatica*, *45*(7), 1659–1667.

Chen, G., Wang, X., & Li, X. (2013). *Fundamentals of complex networks*. Hoboken: Wiley.

Chen, G. R. (2014). Problems and challenges in control theory under complex dynamical network environments. *Acta Automatica Sinica*, *39*(4), 312–321.

Costa, Ld F, Rodrigues, F. A., Travieso, G., & Villas Boas, P. R. (2007). Characterization of complex networks: A survey of measurements. *Advances in Physics*, *56*(1), 167–242.

Cowan, N. J., Chastain, E. J., Vilhena, D. A., Freudenberg, J. S., & Bergstrom, C. T. (2012). Nodal dynamics, not degree distributions, determine the structural controllability of complex networks. *PLoS ONE*, *7*(6), e38398.

Cruz, M Ad R, & Rocha, H. R. O. (2017). Planning metering for power distribution systems monitoring with topological reconfiguration.

Journal of Control, Automation and Electrical Systems, *28*, 135–146.

Derakhshan, F., & Yousefi, S. (2019). A review on the applications of multiagent systems in wireless sensor networks. *International Journal of Distributed Sensor Networks*, *15*(5)

Dorfler, F., & Bullo, F. (2014). Synchronization in complex networks of phase oscillators: A survey. *Automatica*, *50*(6), 1539–1564.

Dorfler, F., Chertkov, M., & Bullo, F. (2013). Synchronization in complex oscillator networks and smart grids. *PNAS*, *110*(6), 2005–2010.

Eroglu, D., Lamb, J. S., & Pereira, T. (2017). Synchronisation of chaos and its applications. *Contemporary Physics*, *58*(3), 207–243.

Fortunato, S. (2010). Community detection in graphs. *Physics Reports*, *486*(3–5), 75–174.

Friedland, B. (1975). Controllability index based on conditioning number. *Journal of Dynamic Systems, Measurement, and Control*, *97*(4), 444–445.

Fu, Y., Wang, L., & Chen, M. (2016). Robustness of controllability for scale-free networks based on a nonlinear load-capacity model. *IFAC Proceedings Volumes*, *49*(4), 37–42.

Gao, J., Liu, Y. Y., D'Souza, R. M., & Barabási, A. L. (2014). Target control of complex networks. *Nature Communications*, *5*, 5415.

Gates, A. J., & Rocha, L. M. (2015). Control of complex networks requires both structure and dynamics. *Scientific Reports*, *6*, 24456.

Gilarranz, L. J., Rayfield, B., Liñán-Cembrano, G., Bascompte, J., & Gonzalez, A. (2017). Effects of network modularity on the spread of perturbation impact in experimental metapopulations. *Science*, *357*, 199–201.

Gu, S., Pasqualetti, F., Cieslak, M., Telesford, Q. K., Yu, A. B., Kahn, A. E., et al. (2015). Controllability of structural brain networks. *Nature Communications*, *6*, 8414.

Guan, J., Berry, T., & Sauer, T. (2018). Limits on reconstruction of dynamical networks. *Physical Review E*, *98*, 022318.

Guan, Y., & Wang, L. (2018). Controllability of multi-agent systems with directed and weighted signed networks. *Systems and Control Letters*, *116*, 47–55.

Gutiérrez, R., Sendiña-Nadal, I., Zanin, M., Papo, D., & Boccaletti, S. (2012). Targeting the dynamics of complex networks. *Scientific reports*, *2*, 396.

Haber, A., & Verhaegen, M. (2014). Subspace identification of large-scale interconnected systems. *IEEE Transactions on Automatic Control*, *59*(10), 2754–2759.

Haber, A., Molnar, F., & Motter, A. E. (2018). State observation and sensor selection for nonlinear networks. *IEEE Transactions on Control of Network Systems*, *5*(2), 694–708.

Hammond, C., Bergman, H., & Brown, P. (2007). Pathological synchronization in Parkinson's disease: Networks, models and treatments. *Trends in Neurosciences*, *30*(7), 357–364.

Hermann, R., & Krener, A. J. (1977). Nonlinear controllability and observability. *IEEE Transactions on Automatic Control*, *22*(5), 728–740.

Hieu, T., & Tyrone, F. (2012). *Functional observers for dynamical systems*. Berlin: Springer.

Iudice, F. L., Sorrentino, F., & Garofalo, F. (2019). On node controllability and observability in complex dynamical networks. *IEEE Control Systems Letters*, *3*(4), 847–852.

Jennings, L. S., Fernando, T. L., & Trinh, H. M. (2011). Existence conditions for functional observability from an eigenspace perspective. *IEEE Transactions on Automatic Control*, *56*(12), 2957–2961.

Jia, T., Liu, Y. Y., Csoka, E., Posfai, M., Slotine, J. J., & Barabási, A. L. (2013). Emergence of bimodality in controlling complex networks. *Nature Communications*, *4*, 2002.

Jiang, J., & Ying-Cheng, Lai. (2019). Irrelevance of linear controllability to nonlinear dynamical networks. *Nature Communications*, *10*, 3961.

Johnson, C. D. (1969). Optimization of a certain quality of complete controllability and observability for linear dynamical systems. *Journal of Basic Engineering*, *91*(2), 228–238.

Kalman, R. (1959). On the general theory of control systems. *IRE Transactions on Automatic Control*, *4*(3), 110–110.

Khalil, H. K. (2002). *Nonlinear systems* (3rd ed.). Upper Saddle River: Prentice Hall.

Klaus, R., & Reinschke, K. J. (1999). An efficient method to compute Lie derivatives and the observability matrix for nonlinear systems. In *International Symposium on Nonlinear Theory and its Applications (NOLTA)* 2

Komareji, M., & Bouffanais, R. (2014). Controllability of a swarm of topologically interacting autonomous agents. *Internation Journal of Complex Systems in Science*, *3*(1), 11–19.

Kuramoto, Y. (1975). Self-entrainment of a population of coupled non-linear oscillators. In *International symposium on mathematical problems in theoretical physics* (pp. 420–422)

Laschov, D., Margaliot, M., & Even, G. (2013). Observability of Boolean networks: A graph-theoretic approach. *Automatica*, *49*(8), 2351–2362.

Leitold, D., Vathy-Fogarassy, A., & Abonyi, J. (2017). Controllability and observability in complex networks—The effect of connection types networks. *Scientific Reports*, *7*, 151.

Leitold, D., Vathy-Fogarassy, A., & Abonyi, J. (2019). Network-based observability and controllability analysis of dynamical systems: The NOCAD toolbox. *F1000Research*, *8*, 646.

Letellier, C., & Aguirre, L. A. (2002). Investigating nonlinear dynamics from time series: The influence of symmetries and the choice of observables. *Chaos*, *12*(3), 549–558.

Letellier, C., & Aguirre, L. A. (2009). Symbolic observability coefficients for univariate and multivariate analysis. *Physical Review E*, *79*, 066210.

Letellier, C., Maquet, J., Sceller, L. L., Gouesbet, G., & Aguirre, L. A. (1998). On the non-equivalence of observables in phase-space reconstructions from recorded time series. *Journal of Physics A: Mathematical and General*, *31*, 7913–7927.

Letellier, C., Aguirre, L. A., & Maquet, J. (2005). Relation between observability and differential embeddings for nonlinear dynamics. *Physical Review E*, *71*, 066213.

Letellier, C., Sendiña-Nadal, I., & Aguirre, L. A. (2018). A nonlinear graph-based theory for dynamical network observability. *Physical Review E*, *98*, 020303.

Li, A., Cornelius, S. P., Liu, Y. Y., Wang, L., & Barabási, A. L. (2017). The fundamental advantages of temporal networks. *Science*, *358*, 1042–1046.

Li, J., Chen, X., Pequito, S., Pappas, G. J., & Preciado, V. M. (2019). Resilient structural stabilizability of undirected networks. In *2019 American Control Conference (ACC)* (pp. 5173–5178).

Lin, C. T. (1974). Structural controllability. *IEEE Transactions on Automatic Control*, *19*(3), 201–208.

Liu, Y. Y., & Barabási, A. L. (2016). Control principles of complex systems. *Reviews of Modern Physics*, *88*, 035006.

Liu, Y. Y., Slotine, J. J., & Barabási, A. L. (2011). Controllability of complex networks. *Nature*, *473*, 167–73.

Liu, Y. Y., Slotine, J. J., & Barabási, A. L. (2013). Observability of complex systems. *PNAS*, *110*(7), 2460–2465.

Lombardi, A., & Hörnquist, M. (2007). Controllability analysis of networks. *Physical Review E*, *75*, 056110.

Lu, Z., Zhang, L., & Wang, L. (2017). Observability of multi-agent systems with switching topology. *IEEE Transactions on Circuits and Systems II: Express Briefs*, *64*(11), 1317–1321.

Luan, X., & Tsvetkov, P. V. (2019). Novel consistent approach in controllability evaluations of point reactor kinetics models. *Annals of Nuclear Energy*, *131*, 496–506.

Luenberger, G. (1966). Observers for multivariable systems. *IEEE Transactions on Automatic Control AC-I*, *I*(2), 190–197.

Malik, O. P. (2013). Evolution of power systems into smarter networks. *Journal of Control, Automation and Electrical Systems*, *24*, 139–147.

Mesbahi, A., Bu, J., & Mesbahi, M. (2019). Nonlinear observability via koopman analysis: Characterizing the role of symmetry. arXiv:1904.08449 [csSY]

Montanari, A. N. (2019). Observability of Dynamical Networks. Ph.D. thesis (in work), Universidade Federal de Minas Gerais

Montanari, A. N., & Aguirre, L. A. (2019). Particle filtering of dynamical networks: Highlighting observability issues. *Chaos*, *29*, 033118.

Monteiro, L. H. A. (2014). *Sistemas Dinâmicos Complexos* (2nd ed.). Rio de Janeiro: Editora Livraria de Física.

Monticelli, A., & Wu, F. F. (1985). Network observability: Theory. *IEEE Transactions on Power Apparatus and Systems PAS-*, *104*(5), 1042–1048.

Moreira, E. I., & Aguirre, L. A. (2019). Resiliência de Sistemas Elétricos de Potência Representados por Redes de Kuramoto. In *14° Simpósio Brasileiro de Automação Inteligente (SBAI)*

Moreno, Y., & Pacheco, F. (2004). Synchronization of Kuramoto oscillators in scale-free networks. *Europhysics Letters*, *68*(4), 603–609.

Moreno, Y., Pastor-Satorras, R., & Vespignani, A. (2002). Epidemic outbreaks in complex heterogeneoeus networks. *European Physical Journal B*, *26*(4), 521–529.

Motter, A. E. (2015). Networkcontrology. *Chaos*, *25*, 097621.

Nacher, J. C., & Akutsu, T. (2013). Structural controllability of unidirectional bipartite networks. *Scientific Reports*, *3*, 1647.

Nakao, H., & Mikhailov, A. S. (2010). Turing patterns in network-organized activator-inhibitor systems. *Nature Physics*, *6*, 544–550.

Nemhauser, G., Wolsey, L., & Fisher, M. (1978). An analysis of approximations for maximizing submodular set functions-I. *Mathematical Programming*, *14*(1), 265–294.

Nepusz, T., & Vicsek, T. (2012). Controlling edge dynamics in complex networks. *Nature Physics*, *8*, 568–573.

Newman, M. (2010). *Networks: An introduction* (1st ed.). Oxford: OUP.

Nishikawa, T., & Motter, A. E. (2015). Comparative analysis of existing models for power-grid synchronization. *New Journal of Physics*, *17*, 015012.

Notarstefano, G., & Parlangeli, G. (2013). Controllability and observability of grid graphs via reduction and symmetries. *IEEE Transactions on Automatic Control*, *58*(7), 1719–1731.

Olfati-Saber, R. (2006). Flocking for multi-agent dynamic systems: Algorithms and theory. *IEEE Transactions on Automatic Control*, *51*(3), 401–420.

Olshevsky, A. (2014). Minimal controllability problems. *IEEE Transactions on Control of Network Systems*, *1*(3), 249–258.

O'Reilly, J. (1983). *Observers for linear systems* (1st ed.). Cambridge: Academic Press.

Overschee, P., & De Moor, B. (1996). *Subspace identification for linear systems* (1st ed.). New York: Springer.

Pang, S. P., Wang, W. X., Hao, F., & Lai, Y. C. (2017). Universal framework for edge controllability of complex networks. *Scientific Reports*, *7*, 4224.

Parlangeli, G., & Notarstefano, G. (2012). On the reachability and observability of path and cycle graphs. *IEEE Transactions on Automatic Control*, *57*(3), 743–748.

Pasqualetti, F., Zampieri, S., & Bullo, F. (2013). Controllability, limitations and algorithms for complex networks. *IEEE Transactions on Control of Network Systems*, *1*(1), 40–52.

Pasqualetti, F., Favaretto, C., Zhao, S., & Zampieri, S. (2018). Fragility and controllability tradeoff in complex networks. In *2018 Annual American control conference (ACC)* (pp. 216–221).

Pearce, D. J., Miller, A. M., Rowlands, G., & Turner, M. S. (2014). Role of projection in the control of bird flocks. *Proceedings of the National Academy of Sciences of the United States of America*, *111*(29), 10422–10426.

Pecora, L. M., & Carroll, T. L. (1990). Synchronization in chaotic systems. *Physical Review Letters*, *64*(8), 821–824.

Pecora, L. M., & Carroll, T. L. (1998). Master stability functions for synchronized coupled systems. *Physical Review Letters*, *80*(10), 2109–2112.

Peng, J., Sun, Y., & Wang, H. F. (2006). Optimal PMU placement for full network observability using Tabu search algorithm. *International Journal of Electrical Power and Energy Systems*, *28*(4), 223–231.

Phadke, A., & Thorp, J. (2008). *Synchronized phasor measurements and their applications* (1st ed.). New York: Springer.

Pósfai, M., Liu, Y. Y., Slotine, J. J., & Barabási, A. L. (2013). Effect of correlations on controllability transition in network control. *Scientific Reports*, *3*, 1067.

Pu, C. L., Pei, W. J., & Michaelson, A. (2012). Robustness analysis of network controllability. *Physica A: Statistical Mechanics and its Applications*, *391*(18), 4420–4425.

Qi, J., Sun, K., & Kang, W. (2015). Optimal PMU placement for power system dynamic state estimation by using empirical observability gramian. *IEEE Transactions on Power Systems*, *30*(4), 2041–2054.

Rahmani, A., Ji, M., Mesbahi, M., & Egerstedt, M. (2009). Controllability of multi-agent systems from a graph-theoretic perspective. *SIAM Journal on Control and Optimization*, *48*(1), 162–186.

Rocha, H. R. O., Silva, J. A., de Souza, J. C., & Do Coutto Filho, M. B. (2018). Fast and flexible design of optimal metering systems for power systems monitoring. *Journal of Control, Automation and Electrical Systems*, *29*(2), 209–218.

Rodrigues, F. A., Peron, T. K., Ji, P., & Kurths, J. (2016). The Kuramoto model in complex networks. *Physics Reports*, *610*, 1–98.

Rössler, O. E. (1976). An equation for continuous chaos. *Physics Letters*, *57*(5), 397–398.

Ruths, J., & Ruths, D. (2014). Control profiles of complex networks. *Science*, *343*(6177), 1373–1376.

Sauer, P. W., Pai, M. A., & Chow, J. H. (2017). *Power system dynamics and stability: With synchrophasor measurement and power system toolbox* (2nd ed.). Hoboken: Wiley.

Schäfer, B., Witthaut, D., Timme, M., & Latora, V. (2018). Dynamically induced cascading failures in power grids. *Nature Communications*, *9*, 1975.

Schimit, P. H. T., & Monteiro, L. H. A. (2009). On the basic reproduction number and the topological properties of the contact network: An epidemiological study in mainly locally connected cellular automata. *Ecological Modelling*, *220*(7), 1034–1042.

Singh, A. K., & Hahn, J. (2005). Determining optimal sensor locations for state and parameter estimation for stable nonlinear systems. *Industrial and Engineering Chemistry Research*, *44*(15), 5645–5659.

Slotine, J. J., & Liu, Y. Y. (2012). Complex networks: The missing link. *Nature Physics*, *8*(7), 512–513.

Slutsker, I. W., & Scudder, J. M. (1987). Network observability analysis through measurement jacobian matrix reduction. *IEEE Transactions on Power Systems*, *2*(2), 331–336.

Sontag, E. D. (1991). Kalman's controllability rank condition: From linear to nonlinear. In A. C. Antoulas (Ed.), *Mathematical system theory: The influence of R. E. Kalman* (pp. 453–462). Berlin: Springer.

Stankovski, T., Pereira, T., McClintock, P. V., & Stefanovska, A. (2017). Coupling functions: Universal insights into dynamical interaction mechanisms. *Reviews of Modern Physics*, *89*, 045001.

Su, F., Wang, J., Li, H., Deng, B., Yu, H., & Liu, C. (2017). Analysis and application of neuronal network controllability and observability. *Chaos*, *27*, 023103.

Summers, T. H., Cortesi, F. L., & Lygeros, J. (2016). On submodularity and controllability in complex dynamical networks. *IEEE Transactions on Control of Network Systems*, *3*(1), 91–101.

Sun, J., & Motter, A. E. (2013). Controllability transition and nonlocality in network control. *Physical Review Letters*, *110*, 208701.

Takens, F. (1981). Detecting strange attractors in turbulence. In D. Rand & L. Young (Eds.), *Dynamical systems and turbulence* (pp. 366–381). Berlin: Springer.

Tanner, H. (2004). On the controllability of nearest neighbor interconnections. In *43rd IEEE conference on decision and control* (pp. 2467–2472)

Vk, Tran, & Hs, Zhang. (2018). Optimal PMU placement using modified greedy algorithm. *Journal of Control, Automation and Electrical Systems*, *29*(1), 99–109.

Vicsek, T., Czirok, A., Ben-Jacob, E., Cohen, I., & Shochet, O. (1995). Novel type of phase transition in a system of self-driven particles. *Physical Review Letters*, *75*(6), 1226–1229.

Vidyasagar, M. (1978). *Nonlinear Systems Analysis* (2nd ed.). : Prentice Hall.

Vittal, V. (1992). Transient stability test systems for direct stability methods. *IEEE Transactions on Power Systems*, *7*(1), 37–43.

Vivek, S., Yanni, D., Yunker, P. J., & Silverberg, J. L. (2019). Cyberphysical risks of hacked internet-connected vehicles. *Physical Review E*, *100*, 012316.

Wang, L. Z., Chen, Y. Z., Wang, W. X., & Lai, Y. C. (2017). Physical controllability of complex networks. *Scientific Reports*, *7*, 40198.

Wang, X. F., & Chen, G. (2002). Synchronization in scale-free dynamical networks: Robustness and fragility. *IEEE Transactions on Circuits and Systems I: Fundamental Theory and Applications*, *49*(1), 54–62.

Wang, X. F., & Chen, G. (2003). Complex networks: Small-world, scale-free and beyond. *IEEE Circuits and Systems Magazine*, *3*(1), 6–20.

Watts, D. J., & Strogatz, S. H. (1998). Collective dynamics of 'small-world' networks. *Nature*, *393*, 440–442.

Whalen, A. J., Brennan, S. N., Sauer, T. D., & Schiff, S. J. (2015). Observability and controllability of nonlinear networks: The role of symmetry. *Physical Review X*, *5*, 011005.

Willems, J. L. (1986). Structural controllability and observability. *Systems and Control Letters*, *8*, 5–12.

Wolfrum, M. (2012). The Turing bifurcation in network systems: Collective patterns and single differentiated nodes. *Physica D: Nonlinear Phenomena*, *241*(16), 1351–1357.

Yan, G., Ren, J., Lai, Y. C., Lai, C. H., & Li, B. (2012). Controlling complex networks: How much energy is needed? *Physical Review Letters*, *108*(21), 218703.

Yan, G., Tsekenis, G., Barzel, B., Jj, Slotine, Yy, Liu, & Barabási, A. L. (2015). Spectrum of controlling and observing complex networks. *Nature Physics*, *11*(9), 779–786.

Yang, Y., Wang, J., & Motter, A. E. (2012). Network observability transitions. *Physical Review Letters*, *109*, 258701.

Yuan, Z., Zhao, C., Di, Z., Wang, W. X., & Lai, Y. C. (2013). Exact controllability of complex networks. *Nature Communications*, *4*, 2447.

Zabczyk, J. (1995). *Mathematical control theory: An introduction* (2nd ed.). Boston: Birkhäuser.

Zhang, W., Pei, W., & Guo, T. (2014). An efficient method of robustness analysis for power grid under cascading failure. *Safety Science*, *64*, 121–126.

Zhao, S., & Pasqualetti, F. (2019). Networks with diagonal controllability Gramian: Analysis, graphical conditions, and design algorithms. *Automatica*, *102*, 10–18.

Zhirabok, A., & Shumsky, A. (2012). An approach to the analysis of observability and controllability in nonlinear systems via linear methods. *International Journal of Applied Mathematics and Computer Science*, *22*(3), 507–522.